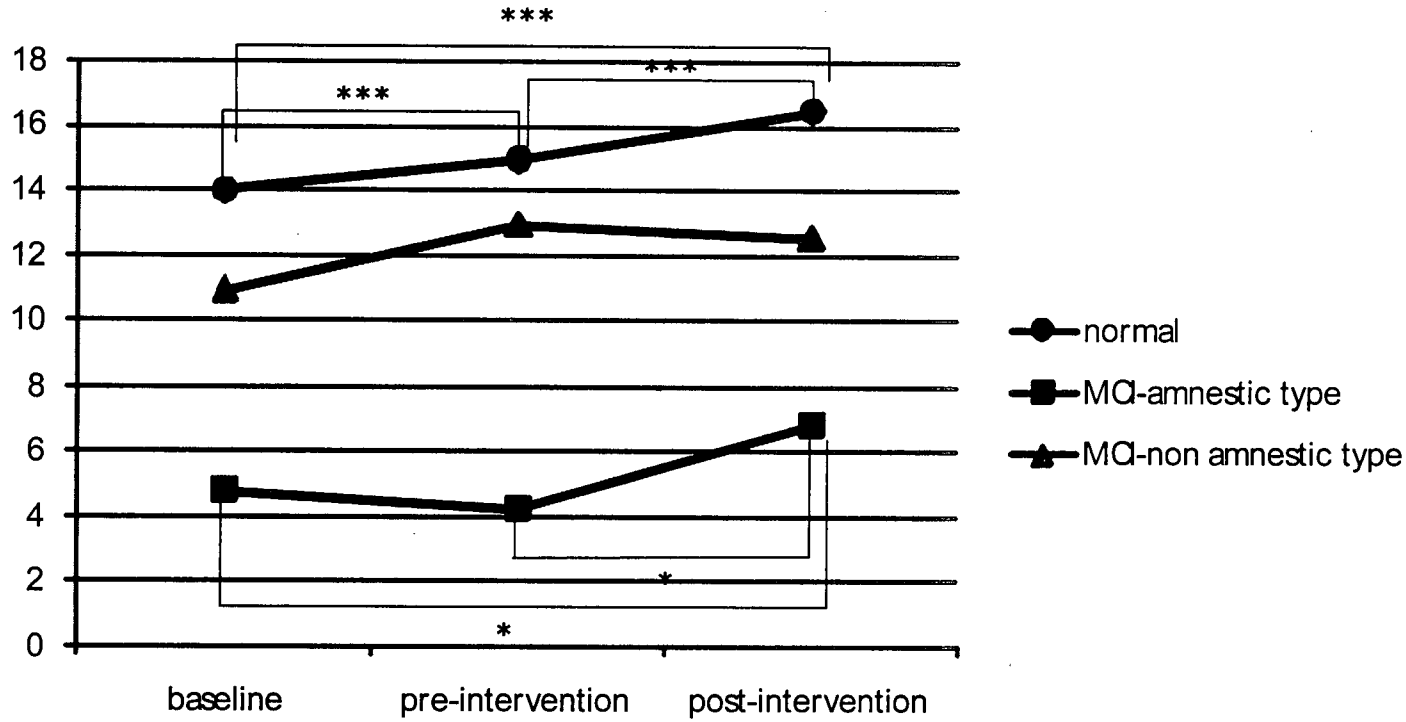

図-1. 健常群, MCI-amnestic 群, MCI-non amnestic 群における認知機能の 2 年間の推移

* p < .05; ** P < .01; *** p < .001

Data Analysis

Statistical analysis were conducted using a statistical software package (SPSS 15.0; SPSS Inc). Demographic data that were continuous in nature were analyzed using analysis of variance, and categorical data were analyzed using χ^2 statistics. Pairwise group comparisons were considered statistically significant if $p < .05$ after Bonferroni adjustment for multiple comparisons. Cognitive and physical measures were analyzed using general linear models in which the diagnostic group was entered as a fixed effect, with age, years of education and sex included as covariates. Pairwise group comparisons were considered statistically significant if $p < .05$ after Bonferroni adjustment for multiple comparisons.

Laterality and aging of thalamic subregions measured by diffusion tensor imaging

Miho Ota[a,c], Takayuki Obata[a,b], Yoshihide Akine[a], Hiroshi Ito[a], Ryohei Matsumoto[a], Hiroo Ikehira[b], Takashi Asada[d] and Tetsuya Suhara[a]

[a]Molecular Neuroimaging Group, [b]Department of Biophysics, Molecular Imaging Center, National Institute of Radiological Sciences, Anagawa, Inage-ku, Chiba, [c]Comprehensive Human Sciences, Medical Sciences for Control of Pathological Processes, Clinical Neuroscience, University of Tsukuba Graduate School and [d]Department of Psychiatry, University of Tsukuba, Tsukuba, Japan

Correspondence to Takayuki Obata, MD, PhD, Department of Biophysics, Molecular Imaging Center, National Institute of Radiological Sciences, 4-9-1 Anagawa, Inage-ku, Chiba 263-8555, Japan
Tel: +81 43 206 3406; fax: +81 43 206 0818; e-mail: t_obata@nirs.go.jp

Received 22 March 2007; accepted 31 March 2007

Thalamic nuclei are comprised of fibers connecting associated cortical regions, and abnormalities of the thalamus are correlated with abnormalities in cognition and behavior. Some previous studies showed the laterality of the whole thalamus and the regional differences among thalamic nuclei. This led us to assess regional characteristics in five major subregions of both sides of the thalamus using diffusion-tensor imaging. Statistically significant lateralities and regional differences were found among the thalamic subregions. Age has a significant correlation with diffusion-tensor imaging metrics where their projection areas are thought to be vulnerable to normal aging. Our results confirmed that the thalamic subregions behave independently, and their respective microstructures warrant further investigations. *NeuroReport* 18:1071–1075 © 2007 Lippincott Williams & Wilkins.

Keywords: aging, fractional anisotropy, mean diffusivity, projection area, thalamic subregion

Introduction

As the central relay station for the brain, the thalamus mediates communication among memory, articulation, consciousness, motor, attention, perception, and the integration of thought processes [1–3]. The multiple functional pathways that relay through the thalamus form the thalamic microstructure. The thalamic microstructure is divided into functionally specific clusters referred to as nuclei. Each of the nuclei of the thalamus has a unique set of projections with different functional implications [2,3].

Using magnetic resonance imaging (MRI), the morphology of the thalamus has been studied. Thalamic changes have been implicated in a large number of diseases and also in normal aging effects [4–6]. The gross morphology of the thalamus revealed on conventional MRI, however, does not necessarily reflect the underlying quality of tissue in its microstructure. Tissue quality is assessable by diffusion tensor imaging (DTI) [7]. DTI allows white matter tracts to be imaged *in vivo* and provides measures of both mean diffusivity (MD) and fractional anisotropy (FA) [8]. Degeneration of white matter tracts would be expected to result in a reduction in FA owing to a loss of directionality of diffusion as well as in an increment in MD owing to diffusivity being averaged in all spatial directions as a result of the loss of myelin and axonal membranes, possibly secondary to Wallerian degeneration [9].

There have been several reports on the topic of the thalamus and aging, and laterality measured with DTI [9–14]. Almost all studies, however, depended on assessment using regions of interest (ROIs) placed visually in the center of the thalamus, and few studies have been done on regional differences of the microstructure. Characterization of the patterns of microstructure deterioration of both sides of thalamus subregions occurring in healthy participants and normal aging would provide important information for research and clinical practice. In this study, we investigated the lateralities and age-related changes of FA and MD in five major subregions of the left and right thalamus using ROI analysis.

Materials and methods

Participants

Twenty-eight healthy right-handed men (mean age 41.3 ± 18.2 years, range 21–71 years; 20–40 years, $n = 16$; 41–60, $n = 6$; 60–71, $n = 6$) participated in this study. The participants partially overlapped with those in the previous report [15]. Conventional MR images of all participants were acquired to exclude brain morphometric abnormalities. Participants with neurological illness, head trauma, loss of consciousness, or psychiatric disorder were also excluded. This study was approved by the Ethics and Radiation Safety Committees of the National Institute of Radiological Sciences, Chiba, Japan. All participants gave their written informed consent.

Diffusion tensor imaging data acquisition and processing

Images were acquired using a Philips Intera, 1.5 tesla MR unit (Philips Medical Systems, Best, The Netherlands). MR data acquisition and DTI calculation were performed in the

same way as previously described [15]. We analyzed MR data sets using DtiStudio (H. Jiang, S. Mori; Johns Hopkins University, Baltimore, Maryland, USA) after all diffusion-weighted images were visually inspected for apparent artifacts owing to subject motion and instrument malfunction. From $b=0$ and six diffusion weighted images, six maps of the apparent diffusion coefficient (ADC) were calculated. Solving six simultaneous equations with respect to ADC_{xx}, ADC_{xy}, etc., yielded the elements of the diffusion tensor. The diffusion tensor was then diagonalized, yielding eigenvalues λ_1, λ_2 and λ_3, as well as eigenvectors that define the predominant diffusion orientation. On the basis of the eigenvalues, FA and MD were calculated on a voxel-by-voxel basis [8].

To exclude some of the subjectivity involved in defining thalamic subregions, we placed subregional ROIs on a standard image, and the ROIs were then placed on all of the individual images normalized to the standard space. On the occasion of normalization, $b=0$ image was first normalized to the Montreal Neurological Institute (MNI) 152-subject T2 template, the standard MNI space, using statistical parametric mapping (SPM2) (Wellcome Department of Imaging Neuroscience, London, UK), and then the transformation matrix was applied to the FA, MD, and eigenvalue maps to normalize them to the standard MNI space. All images were resampled with a final voxel size of $2 \times 2 \times 2$ mm. Further, to avoid the effect of diffusivity of cerebrospinal fluid (CSF), the images of FA, MD, and eigenvalues were masked with the CSF image derived from the segmented $b=0$ image using SPM2. Then, each map was spatially smoothed using a 5 mm full width at half maximum Gaussian Kernel to decrease spatial noise and compensate for the inexact nature of normalization following the 'rule of thumb' as developed for functional MRI and positron emission tomography studies [16].

We separately investigated FA, MD, and eigenvalues in five major subregions of the thalamus using ROI analysis. ROIs for five operationally defined subregions of the thalamus of each hemisphere were defined on the standard brain of the SPM2, avg152T1.mnc image, according to a manual tracing technique described in the literature and applied previously for the study of the thalamus [17,18]. In the first step, we identified the boundaries of the whole thalamus. The mamillary body was used as the anterior boundary. The internal capsule was the lateral boundary, the third ventricle the medial boundary, and the superior border of the midbrain the inferior boundary. The posterior boundary was the location where the hemispheres of the thalamus merged under the crux fornix. The superior boundary was the main body of the lateral ventricle. Second, the thalamus was divided into five distinct subregions. The thalamus was first divided into medial and lateral parts. A line drawn parallel to the lateral border of the midbrain, the interhemispheric fissure, and the cerebral aqueduct represented the vertical bisection. Then, two horizontal lines at 20 and 60% of the vertical line length were drawn to divide the thalamus into six regions. The posterior two regions were combined as the pulvinar. The divisions roughly reflected the individual nuclei located in these thalamic regions.

Statistical analysis

Statistical analyses were performed with SPSS for Windows 11.0.1.j (SPSS Inc., Chicago, Illinois, USA). First, we evaluated the differences between left and right sides and among the subregions [anterior lateral (AL), anterior medial (AM), central lateral (CL), central medial (CM) and posterior] of the thalamus for FA and MD values using two-way factorial analysis of variance in participants under 40 years of age to eliminate the aging effect (16 men of 28 participants, 27.5 ± 6.1 years). A corrected P value less than 0.05 was interpreted as being statistically significant. We also evaluated the differences between left and right sides of the whole thalamus using Student's t-test. A P value less than 0.05 was interpreted as being statistically significant.

Second, the relationships of FA, MD, and eigenvalues of the thalamus subregions with age were evaluated by Pearson's correlation method in all participants. A P value less than 0.005 ($=0.05/10$) was considered significant.

Results

Significant differences were found between the sides of the thalamus and among the subregions in MD ($F=246.9$, $df=1$, $P<0.001$; $F=37.9$, $df=4$, $P<0.001$; interaction: $F=8.5$, $df=4$, $P<0.001$) and FA ($F=35.4$, $df=1$, $P<0.001$; $F=88.7$, $df=4$, $P<0.001$; interaction: $F=1.7$, $df=4$, $P=0.159$), respectively (Table 1). The asymmetry of the whole thalamus was also detected (FA, $P=0.017$; MD, $P<0.001$).

Regional differences of age-related change were observed. The decline in FA showed a significant negative correlation with age in both AM regions (Table 2). The increase in MD showed a significant positive correlation with age in the right AL and both CM and CL subregions (Table 2, Fig. 1). The changes in eigenvalues are summarized in Table 2. The increase in perpendicular diffusivities showed significant positive correlations with age in λ_2 of the right AL subregion and in λ_2 of both CL subregions. No correlations were found between age and the parallel diffusivities.

Discussion

The results of previous studies on the laterality of the thalamus have been less consistent, showing regional differences among the thalamic nuclei [2,3], and laterality

Table 1 Mean right and left fractional anisotropy and mean diffusivity in subregions of thalamus of participants under 40 years ($n=16$)

	AM	AL	CM	CL	Posterior	WT
FA						
Right	0.33±0.03	0.41±0.04	0.28±0.02	0.35±0.03	0.33±0.03	0.34±0.03
Left	0.36±0.03	0.45±0.03	0.29±0.03	0.37±0.03	0.38±0.03	0.37±0.03
MD ($\times 10^{-4}$ mm^2/s)						
Right	8.69±0.44	7.99±0.23	8.16±0.43	7.90±0.13	8.23±0.34	8.19±0.28
Left	7.70±0.41	6.76±0.21	7.54±0.33	7.08±0.30	7.87±0.30	7.39±0.27

AL, anterior lateral region; AM, anterior medial region; CL, central lateral region; CM, central medial region; FA, fractional anisotropy; MD, mean diffusivity; WT; mean value of the whole thalamus.

Table 2 Associations of age with FA, MD, and eigenvalues analyzed by Pearson's correlation coefficient

	AM	AL	CM	CL	Posterior
FA					
Right					
Range	0.17–0.38	0.35–0.52	0.23–0.32	0.30–0.42	0.27–0.41
Correlation coefficients	−0.572	−0.270	−0.153	−0.124	−0.042
P value	0.001*	0.165	0.437	0.529	0.832
Left					
Range	0.25–0.44	0.36–0.52	0.25–0.38	0.29–0.45	0.32–0.42
Correlation coefficients	−0.703	−0.379	−0.181	−0.237	−0.061
P value	<0.001*	0.047	0.357	0.224	0.759
MD					
Right					
Range ($\times 10^{-4}$ mm^2/s)	7.13–9.85	7.58–9.12	7.51–9.22	7.61–8.44	7.54–9.17
Correlation coefficients	0.277	0.550	0.546	0.667	0.200
P value	0.153	0.002*	0.003*	<0.001*	0.308
Left					
Range ($\times 10^{-4}$ mm^2/s)	6.84–9.06	6.34–8.88	6.81–9.13	6.63–8.23	7.24–9.03
Correlation coefficients	0.359	0.423	0.610	0.610	0.442
P value	0.061	0.025	0.001*	0.001*	0.019
λ_1					
Right					
Range ($\times 10^{-4}$ mm^2/s)	8.78–12.64	10.86–12.58	9.66–12.02	10.38–11.53	10.30–12.91
Correlation coefficients	0.034	0.084	0.390	0.355	0.055
P value	0.864	0.671	0.040	0.063	0.779
Left					
Range ($\times 10^{-4}$ mm^2/s)	10.10–12.45	10.49–12.96	9.63–11.25	10.32–12.01	10.69–12.56
Correlation coefficients	−0.284	−0.057	0.495	0.273	0.293
P value	0.143	0.772	0.007	0.160	0.130
λ_2					
Right					
Range ($\times 10^{-4}$ mm^2/s)	6.91–9.85	6.59–8.85	7.28–9.23	7.04–8.17	7.28–9.03
Correlation coefficients	0.331	0.663	0.457	0.634	0.187
P value	0.085	<0.001*	0.015	<0.001*	0.340
Left					
Range ($\times 10^{-4}$ mm^2/s)	7.02–8.85	5.90–7.70	7.39–9.20	6.45–7.73	6.81–8.32
Correlation coefficients	0.250	0.467	0.498	0.658	0.424
P value	0.199	0.012	0.007	<0.001*	0.025
λ_3					
Right					
Range ($\times 10^{-4}$ mm^2/s)	5.11–6.77	3.89–5.47	5.29–6.99	4.68–6.06	4.70–7.10
Correlation coefficients	0.403	0.287	0.395	0.341	0.193
P value	0.033	0.139	0.038	0.076	0.326
Left					
Range ($\times 10^{-4}$ mm^2/s)	4.48–6.56	3.64–5.61	4.55–6.61	4.25–5.83	4.64–6.00
Correlation coefficients	0.462	0.384	0.498	0.494	0.351
P value	0.013	0.044	0.007	0.007	0.067

AL, anterior lateral region; AM, anterior medial region; CL, central lateral region; CM, central medial region; FA, fractional anisotropy; MD, mean diffusivity; $N = 28$; SD, standard deviation.
*A *P* value less than 0.005 (= 0.05/10) was considered significant.

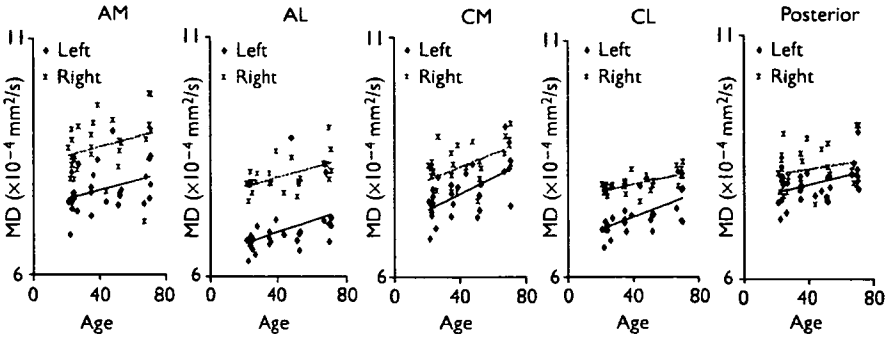

Fig. 1 Scatter diagrams [age versus mean diffusivity (MD)] in subregions [anterior medial (AM), anterior lateral (AL), central medial (CM), central lateral (CL) and Posterior] of thalamus of 28 participants.

between the left and right sides [9,14], as well as no changes between left and right whole thalamus [10–12,19]. In this study, we first evaluated the lateralities and regional differences of the thalamic subregion microstructures. The lower MD in the left thalamus corresponds well with previous studies [9,14]. Recent neuroimaging study has demonstrated larger left than right gray matter volume in various regions [6], and it is sometimes suggested that there is laterality of the areas related to cognitive function [20]. Accordingly, the subregional microstructures of the thalamus, the central relay station for the brain, can be assumed to be asymmetrical.

It was also shown that there were age-related changes of MD [10], ADC [12], and FA [11]. According to those studies, a significant difference in ADC between the right and left thalamus was seen only in participants over 60 years, not in the group under age 60 years, and there were significant differences in both thalamic ADCs between the under 60 years and over 60 years groups [13]. This could be ascribed to the fact that the steeper change in the right thalamus might emphasize the laterality of the over 60 group. In this study, we evaluated the asymmetrical changes of the microstructure occurring in normal aging, and we found that there were steeper changes with age in some of the right thalamic subregions than in the left thalamus, consistent with previous results. Left AM had no correlation with normal aging, so our results suggest that the two sides of thalamic nuclei behave independently, and we should evaluate the microstructure of the thalamic nuclei in a respective manner.

We found the aging effect on FA in both AM subregions, on MD in the right AL subregion and both CM and CL subregions corresponding to the frontal and pre and postcentral gyrus [2], where age-related gray matter volume loss and decline in FA are observed [6,21]. A correlation was reported between right posterior thalamic FA and visuospatial attention [1], and centers of functional activation within the thalamus during motor or executive tasks colocalize within the atlas regions showing high probabilities of connection to motor or prefrontal cortices, respectively [3]. It was also reported that after middle cerebral artery infarcts, an increase in diffusion was observed with DTI in the ipsilateral thalamus [22], and neuronal loss within the ipsilateral thalamus using postmortem material [23]. From these results, we suppose that fewer cortical neurons could be associated with fewer thalamic fibers, and that the changes in FA and MD in the thalamic subregions might imply degeneration of the respective projection areas. In this study, we did not detect any significant change in MD or FA in the two posterior subregions. These results may reflect the low sensibility to aging of the occipital lobe structure [6]. These projection areas may obscure the aging effect on FA and MD in these subregions. In addition, our study showed that the observed increase in MD was due to an increase in perpendicular diffusivity, with a lack of change in parallel diffusivity. These findings are consistent with those of a previous study [11], and a decrease in the number of myelinated neuron fibers with aging is suggested [15].

Aging effects on FA values of subregions were not so clear in this study. This may stem from the fact that the more heterogeneous FA map rather than the relatively uniform MD map cannot be accounted for by standard spatial normalization, especially in the thalamus, which is adjacent to the lateral ventricles [16]. The ventricle with high MD and low FA happened to be spatially normalized and influenced the adjacent area. Our results, however, showed the increase of not only the medial portion but also the lateral portions of thalamus in MD metrics with age. This may indicate that the normalization of relatively uniform MD maps successfully proceeded. This is also relied on the fact that there are thalamic regions with predominantly subcortical connections and only weak or diffuse cortical connections. Directionality of diffusion was obscured for some connections, and we could detect age-related FA change only in the AM subregion that connects a relatively homologous region [2]. The thalamus contains many histologic components other than myelinated axons, such as cell bodies and dendrites, which have a smaller volume than neurons and their myelinated axons [24]. Augmentation of large-diameter fibers and small-volume components may result in the dissociation of FA and MD values [10].

Some limitations exist in this study. We evaluated only men, and numerous sex-associated functional and biological differences in the brain have been described [25]. Further studies, also taking sex differences into account and using the same method, will be necessary. We were unable to delineate and employ an intrathalamic marker as a consistent landmark for our regional subdivisions. Rather, we relied upon approximate percentage-based divisions of the total thalamic area as a means of dividing the thalamus. This automated method reduced some of the subjectivity and systematic bias involved in defining thalamic subareas with limited resolution imaging. Without manual editing, however, the assumptions that all thalamic nuclei are consistently represented by these rigid subdivisions would not be confirmed.

Conclusion

We found that there were significant lateralities and regional differences in thalamic subregions, and that age-related changes were detected in some thalamic subregions where their projection areas are thought to be vulnerable to normal aging. Diffusion asymmetry and regional differences of the aging effect in thalamic subregions have important implications for research and clinical practice, and the two sides of thalamic nuclei would warrant further investigations.

Acknowledgements

This study was supported in part by a Grant-in-Aid for Molecular Imaging Program from the Ministry of Education, Culture, Sports, Science and Technology (MEXT) of the Japanese Government.

References

1. Tuch DS, Salat DH, Wisco JJ, Zaleta AK, Hevelone ND, Rosas HD. Choice reaction time performance correlates with diffusion anisotropy in white matter pathways supporting visuospatial attention. *PNAS* 2005; 102:12212–12217.
2. Behrens TE, Johansen-Berg H, Woolrich MW, Smith SM, Wheeler-Kingshott CA, Boulby PA, *et al.* Non-invasive mapping of connections between human thalamus and cortex using diffusion imaging. *Nat Neurosci* 2003; 6:750–757.
3. Johansen-Berg H, Behrens TE, Sillery E, Ciccarelli O, Thompson AJ, Smith SM, *et al.* Functional-anatomical validation and individual variation of diffusion tractography-based segmentation of the human thalamus. *Cereb Cortex* 2005; 15:31–39.
4. Autti T, Raininko R, Vanhanen SL, Kallio M, Santavuori P. MRI of the normal brain from early childhood to middle age. II. Age dependence of signal intensity changes on T2-weighted images. *Neuroradiology* 1994; 36:649–651.
5. Walhovd KB, Fjell AM, Reinvang I, Lundervold A, Dale AM, Eilertsen DE, *et al.* Effects of age on volumes of cortex, white matter and subcortical

structures. *Neurobiol Aging* 2005; 26:1261–1270. Comment in *Neurobiol Aging* 2005; 26:1271–1274. Discussion 1275–1278.
6. Good CD, Johnsrude I, Ashburner J, Henson RNA, Friston KJ, Frackowiak RSJ. Cerebral asymmetry and the effect of sex and handedness on brain structure: a voxel-based morphometric analysis of 465 normal adult human brains. *Neuroimage* 2001; 14:685–700.
7. Le Bihan D. Molecular diffusion, tissue microdynamics and microstructure. *NMR Biomed* 1995; 8:375–386.
8. Pierpaoli C, Basser PJ. Toward a quantitative assessment of diffusion anisotropy. *Mag Res Med* 1996; 36:893–906. Erratum in: *Magn Reson Med* 1997; 37:972.
9. Kantarci K, Jack CR Jr, Xu YC, Campeau NG, O'Brien PC, Smith GE, *et al.* Mild cognitive impairment and Alzheimer disease: regional diffusivity of water. *Radiology* 2001; 219:101–107.
10. Abe O, Aoki S, Hayashi N, Yamada H, Kunimatsu A, Mori H, *et al.* Normal aging in the central nervous system: quantitative MR diffusion-tensor analysis. *Neurobiol Aging* 2002; 23:433–441.
11. Bhagat YA, Beaulieu C. Diffusion anisotropy in subcortical white matter and cortical gray matter: changes with aging and the role of CSF-suppression. *J Magn Reson Imaging* 2004; 20:216–227.
12. Engelter ST, Provenzale JM, Petrella JR, DeLong DM, MacFall JR. The effect of aging on the apparent diffusion coefficient of normal-appearing white matter. *AJR* 2000; 175:425–430.
13. Naganawa S, Sato K, Katagiri T, Mimura T, Ishigaki T. Regional ADC values of the normal brain: differences due to age, gender, and laterality. *Eur Radiol* 2003; 13:6–11.
14. Fabiano AJ, Horsfield MA, Bakshi R. Interhemispheric asymmetry of brain diffusivity in normal individuals: a diffusion-weighted MR imaging study. *Am J Neuroradiol* 2005; 26:1089–1094.
15. Ota M, Obata T, Akine Y, Ito H, Ikehira H, Asada T. Age-related degeneration of corpus callosum measured with diffusion tensor imaging. *Neuroimage* 2006; 31:1445–1452.
16. Snook L, Plewes C, Beaulieu C. Voxel based versus region of interest analysis in diffusion tensor imaging of neurodevelopment. *Neuroimage* 2007; 34:243–252.
17. Buchsbaum MS, Someya T, Teng CY, Abel L, Chin S, Najafi A, *et al.* PET and MRI of the thalamus in never-medicated patients with schizophrenia. *Am J Psychiatry* 1996; 153:191–199.
18. Gilbert AR, Rosenberg DR, Harenski K, Spencer S, Sweeney JA, Keshavan MS. Thalamic volumes in patients with first-episode schizophrenia. *Am J Psychiatry* 2001; 158:618–624.
19. Snook L, Paulson LA, Roy D, Phillips L, Beaulieu C. Diffusion tensor imaging of neurodevelopment in children and young adults. *Neuroimage* 2005; 26:1164–1173.
20. Nyberg L, McIntosh AR, Houle S, Nilsson LG, Tulving E. Activation of medial temporal structures during episodic memory retrieval. *Nature* 1996; 380:715–717.
21. Sullivan EV, Adalsteinsson E, Hedehus M, Ju C, Moseley M, Lim KO, *et al.* Equivalent disruption of regional white matter microstructure in aging healthy men and women. *NeuroReport* 2001; 12:99–104.
22. Herve D, Molko N, Pappata S, Buffon F, LeBihan D, Bousser MG. Longitudinal thalamic diffusion changes after middle cerebral artery infarcts. *J Neurol Neurosurg Psychiatry* 2005; 76:200–205. Comment in: *J Neurol Neurosurg Psychiatry* 2005; 76:159–160.
23. Ogawa T, Yoshida Y, Okudera T, Noguchi K, Kado H, Uemura K. Secondary thalamic degeneration after cerebral infarction in the middle cerebral artery distribution: evaluation with MRI imaging. *Radiology* 1997; 204:255–262.
24. Percheron G. Thalamus. In: Paxinos G, Mai JK, editors. *The human nervous system. 2nd ed.* San Diego, California: Academic Press; 2003. pp. 592–675.
25. Kaasinen V, Nagren K, Hietala J, Farde L, Rinne JO. Sex differences in extrastriatal dopamine d(2)-like receptors in the human brain. *Am J Psychiatry* 2001; 158:308–311.

Human Molecular Genetics, 2007, Vol. 16, No. 23 *2854–2869*
doi:10.1093/hmg/ddm244
Advance Access published on August 30, 2007

Genetic association of *CTNNA3* with late-onset Alzheimer's disease in females

Akinori Miyashita[1], Hiroyuki Arai[2], Takashi Asada[3], Masaki Imagawa[4], Etsuro Matsubara[5], Mikio Shoji[6], Susumu Higuchi[7], Katsuya Urakami[8], Akiyoshi Kakita[9], Hitoshi Takahashi[9], Shinichi Toyabe[10†], Kohei Akazawa[10], Ichiro Kanazawa[11], Yasuo Ihara[12,‡], Ryozo Kuwano[1*]; The Japanese Genetic Study Consortium for Alzeheimer's Disease

[1]Bioresource Science Branch, Center for Bioresources, Brain Research Institute, Niigata University, Niigata 951-8585, Japan, [2]Department of Geriatrics and Gerontology, Center for Asian Traditional Medicine, Tohoku University Graduate School of Medicine, Sendai 980-8574, Japan, [3]Department of Psychiatry, Institute of Clinical Medicine, University of Tsukuba, Tsukuba 305-8575, Japan, [4]Imagawa Clinic, Fukushima-ku, Osaka 553-0003, Japan, [5]Department of Alzheimer's Disease Research, National Institute for Longevity Sciences, National Center for Geriatrics and Gerontology, Obu 474-8522, Japan, [6]Department of Neurology, Neuroscience and Biophysiological Science, Hirosaki University, School of Medicine, Hirosaki 036-8562, Japan, [7]Division of Clinical Research, Kurihama Alcoholism Center, National Hospital Organization, Yokosuka 239-0841, Japan, [8]Department of Biological Regulation, Section of Environment and Health Science, Faculty of Medicine, Tottori University, Yonago 683-8503, Japan, [9]Departments of Pathology and Pathological Neuroscience, Brain Research Institute, Niigata University, Niigata 951-8585, Japan, [10]Department of Medical Informatics, Niigata University, Niigata 951-8520, Japan, [11]National Center for Neurology and Psychiatry, Kodaira 187-8502, Japan and [12]Department of Neuropathology, Faculty of Medicine, University of Tokyo, Bunkyo-ku, Tokyo 113-0033, Japan

Received July 18, 2007; Revised and Accepted August 22, 2007

Alzheimer's disease (AD), the most common form of dementia in the elderly, was found to exhibit a trend toward a higher risk in females than in males through epidemiological studies. Therefore, we hypothesized that gender-related genetic risks could exist. To reveal the ones for late-onset AD (LOAD), we extended our previous genetic work on chromosome 10q (genomic region, 60–107 Mb), and single nucleotide polymorphism (SNP)-based genetic association analyses were performed on the same chromosomal region, where the existence of genetic risk factors for plasma Aβ42 elevation in LOAD was implied on a linkage analysis. Two-step screening of 1140 SNPs was carried out using a total of 1408 subjects with the *APOE-ε3*3* genotype: we first genotyped an exploratory sample set (LOAD, 363; control, 337), and then genotyped some associated SNPs in a validation sample set (LOAD, 336; control, 372). Seven SNPs, spanning about 38 kb, in intron 9 of *CTNNA3* were found to show multiple-hit association with LOAD in females, and exhibited more significant association on Mantel–Haenszel test (allelic P-values$_{MH\text{-}F}$ = 0.000005945–0.0007658). Multiple logistic regression analysis of a total of 2762 subjects (LOAD, 1313; controls, 1449) demonstrated that one of the seven SNPs directly interacted with the female gender, but not with the male gender. Furthermore, we found that this SNP exhibited no interaction with the *APOE-ε4* allele. Our data suggest that *CTNNA3* may affect LOAD through a female-specific mechanism independent of the *APOE-ε4* allele.

*To whom correspondence should be addressed at: 1-757 Asahimachi, Chuo-ku, Niigata 951-8585, Japan. Tel: +81 252272343; Fax: +81 252270793; Email: ryosun@bri.niigata-u.ac.jp
†Present address: Risk Management Office, Niigata University Medical and Dental Hospital, Niigata 951-8520, Japan.
‡Present address: Planning Office, Faculty of Life and Medical Sciences, Doshisha University, Kyoto 619-0225, Japan.

INTRODUCTION

Alzheimer's disease (AD) is a neurodegenerative disorder clinically characterized by progressive cognitive deterioration and is the most common form of dementia in the elderly. Its neuropathological features are amyloid plaques [extracellular deposition of amyloid β-protein (Aβ)] and neurofibrillary tangles (intracellular aggregation of highly phosphorylated microtubule-associated protein tau), which finally lead to synaptic loss and/or neuronal death.

Recent epidemiological studies on AD revealed gender-related differences in its prevalence (1–3) and incidence (4–6). Compared with males, females are more likely to develop AD, although results contradicting this gender difference have been reported (7–9). In blood mononuclear cells in AD, there are substantial gender differences in gene expression (10). The plasma level of amyloid beta-protein 42 (Aβ42), a major constituent of senile plaques, is significantly increased in females with mild cognitive impairment, a transitional state between normal aging and mild dementia (11). In transgenic animal models of AD, gender-dependent accumulation and deposition of Aβ42 and Aβ40 have been observed (12–15). Moreover, there has been increasing research on gender-related genetic risk factors in AD: *ACT* (16), *MPO* (17,18), *ACE* (19), *ESR2* (20), *DSC1* (21) and *ABCA1* (22). Therefore, based on these findings, we hypothesized that gender-related genetic risk factors that modify Aβ metabolism in late-onset AD (LOAD), which accounts for 95–99% of AD, could exist.

We have paid a great deal of attention to chromosome 10q, especially because the existence of genetic risk factors for plasma Aβ42 elevation in it was implied on linkage analysis of LOAD families (23). Furthermore, through other genetic approaches, including genome-wide linkage screening of affected sib pairs (24) and candidate gene-based analysis of multiplex AD families (25), chromosome 10q was strongly suggested to be the most prominent one for LOAD. Therefore, regarding a genomic region on chromosome 10q (60–107 Mb), we previously performed large-scale single nucleotide polymorphism (SNP)-based screening of a Japanese population to identify additional genetic risk factors to *APOE* (19q13.2), which is universally recognized as a major risk gene for the development of LOAD (OMIM +107741). Consequently, we found that *DNMBP*, which is involved in synaptic vesicle recycling, was associated with LOAD with the *APOE-ε3*3* genotype or lacking the *APOE-ε4* allele in several sample sets (26).

Interestingly, replicated evidence for a parent-of-origin effect of chromosome 10q was recently reported for LOAD (27,28), which suggests that gender-related genes such as imprinting genes could be responsible for the disease development. Here, in order to determine whether or not gender-related loci associated with LOAD are present, our previous genetic work on chromosome 10q (26) was extended. Two sample sets for screening, *Exploratory* and *Validation*, comprising only *APOE-ε3*3* subjects were prepared, which were used for a case–control association study after being stratified as to gender. We first genotyped the Exploratory set, and then genotyped some significantly associated SNPs in the Validation set. Through this stepwise screening, among the 1140 SNPs subjected to the exploratory screening, we finally found seven SNPs located in intron 9 of *CTNNA3* that showed reproducible association with LOAD in females. These replicated SNPs were further examined by means of genotyping of all the subjects with all *APOE* genotypes (*ε2*2*, *ε2*3*, *ε2*4*, *ε3*3*, *ε3*4* and *ε4*4*), i.e. 1526 LOAD patients (female, 1103; male, 423) and 1666 controls (female, 998; male, 668), some of them exhibiting significance only in a female sub-sample set. In terms of biological functions, *CTNNA3* (29,30), encoding α-T catenin, is thought to be a promising candidate for LOAD because it is a binding partner of β-catenin, which interacts with PSEN1 (31), and because it was recently shown to be associated with the level of plasma Aβ42 in a set of families with LOAD (32). Multiple logistic regression analysis in a total of 2762 subjects (LOAD, 1313; controls, 1449) revealed that one (SNP rs713250) of the seven associated SNPs exhibits a significant interaction with the female gender, but not with the male gender and the *APOE-ε4* allele. Our data suggest that *CTNNA3* could affect LOAD through a female-specific mechanism independent of the *APOE-ε4* allele.

RESULTS

Allelic association

To determine whether gender-related loci associated with LOAD on chromosome 10q (60–107 Mb) exist or not, we stratified the Exploratory sample set (Table 1) by gender, resulting in female and male subsets. An allelic contingency table (2 × 2)-based χ^2 test was performed using already-obtained genotype data (26) for 1140 SNPs for the Exploratory set. Calculation of allelic *P*-values and odds ratios (ORs) with 95% confidence interval (CI) was carried out to examine the genetic association of these SNPs. In a Japanese population, these SNPs were actually polymorphic and showed a *P*-value >0.05 in exact tests of Hardy–Weinberg equilibrium (HWE) in both cases and controls of the Exploratory set (details given under Materials and Methods). The results of χ^2 tests for the gender-stratified sets are presented in Fig. 1. In the female group (LOAD, 249; controls, 223), 106 of the 1140 SNPs had significant allelic *P*-values <0.05, and 34 of these 106 showed more significant values (allelic *P*-values <0.01). In the male group (LOAD, 114; controls, 114), 53 of the 1140 SNPs showed allelic *P*-values <0.05, and 7 of these 53 showed more significant association with allelic *P*-values <0.01.

A total of 41 SNPs (34 and 7 SNPs in female and male Exploratory sets, respectively) showing allelic *P*-values <0.01 were further analyzed by means of χ^2 tests to determine whether or not these SNPs actually exhibit reproducible allelic association using another sample set, Validation, sub-grouped as to gender (Table 1). In the male Validation set (LOAD, 94; controls, 159), three of the above-mentioned seven SNPs showed reproducible association (allelic *P*-values = 0.0342 – 0.046). Among these three SNPs, only SNP rs1000280 exhibited a significant value on Mantel–Haenszel test (allelic $P\text{-value}_{\text{MH-M}} = 0.0009112$). This SNP is located in the intergenic region between *LOXL4* (100.00–100.02 Mb) and *C10orf33* (100.13–100.16 Mb); therefore, we did not

Table 1. Subject information

Sample set ID	Number of subjects		AAO/AAE Mean (SD)	Range	MMSE Mean (SD)	Range	*APOE* Genotype						Allele		
							*2*2*	*2*3*	*2*4*	*3*3*	*3*4*	*4*4*	*ε2*	*ε3*	*ε4*
Overall set															
All	Female														
	LOAD	1103	73.5 (6.6)	60–93	15.7 (7.0)	0–30	0	31	13	491	465	103	44	1478	684
	Control	998	73.0 (7.9)	60–96	28.0 (1.8)	24–30	2	77	9	748	152	10	90	1725	181
	Male														
	LOAD	423	73.3 (6.6)	60–93	18.4 (6.6)	0–30	1	18	4	208	148	44	24	582	240
	Control	668	73.1 (7.7)	60–95	28.1 (1.8)	24–30	1	55	6	495	104	7	63	1149	124
Subsets															
Negative-ε4	Female														
	LOAD	522	74.6 (7.0)	60–93	15.1 (7.4)	0–30	0	31		491			31	1013	
	Control	827	73.1 (7.9)	60–96	28.0 (1.8)	24–30	2	77		748			81	1573	
	Male														
	LOAD	227	73.6 (7.2)	60–93	17.9 (7.3)	0–30	1	18		208			20	434	
	Control	551	73.0 (7.8)	60–95	28.1 (1.8)	24–30	1	55		495			57	1045	
Positive-ε4	Female														
	LOAD	581	72.6 (6.0)	60–92	16.3 (6.6)	0–30			13		465	103	13	465	684
	Control	171	72.7 (7.6)	60–90	28.0 (1.9)	24–30			9		152	10	9	152	181
	Male														
	LOAD	196	72.9 (5.8)	60–86	18.9 (5.7)	1–30			4		148	44	4	148	240
	Control	117	73.7 (7.4)	60–91	27.9 (1.9)	24–30			6		104	7	6	104	124
*ε3*3*	Female														
	LOAD	491	74.7 (7.0)	60–93	15.1 (7.3)	0–30	—	—	—	491	—	—	—	982	
	Control	748	73.1 (7.9)	60–96	28.0 (1.8)	24–30	—	—	—	748	—	—	—	1496	—
	Male														
	LOAD	208	73.7 (7.3)	60–93	18.0 (7.3)	0–30				208				416	
	Control	495	73.0 (7.8)	60–95	28.1 (1.8)	24–30				495				990	
Screening sets															
Exploratory	Female														
	LOAD	249	74.3 (6.2)	62–90	15.7 (7.2)	0–30				249				498	—
	Control	223	80.2 (4.1)	75–96	28.0 (1.9)	24–30	—	—		223	—	—	—	446	
	Male														
	LOAD	114	74.6 (6.8)	62–93	19.2 (7.6)	0–30				114				228	
	Control	114	80.6 (4.0)	75–95	28.0 (2.0)	24–30				114				228	
Validation	Female														
	LOAD	242	75.0 (7.7)	60–93	14.7 (7.3)	0–29				242				484	
	Control	213	75.5 (4.7)	70–94	27.8 (1.9)	24–30	—	—		213				426	
	Male														
	LOAD	94	72.6 (7.6)	60–92	16.8 (6.9)	0–29				94				188	
	Control	159	75.7 (4.5)	70–92	28.1 (1.8)	24–30	—	—	—	159	—	—	—	318	—

The sample set IDs used in this study, i.e. single SNP case–control study, linkage disequilibrium and case–control haplotype analyses, and multiple logistic regression analysis, are shown in italics.

investigate this SNP further. In the female Validation set (LOAD, 242; controls, 213), 16 of the above-mentioned 34 SNPs exhibited allelic association with *P*-values <0.05. These SNPs exhibited significance on Mantel–Haenszel test of the two female sets (allelic $P\text{-values}_{\text{MH-F}} = 0.000005945 - 0.0008809$). These allelic $P\text{-values}_{\text{MH-F}}$ remained at significant levels even after Bonferroni's correction for 34 tests (allelic $P\text{-values}_{\text{MH-F(B)}} = 0.0002021 - 0.02995$). Of the 16 SNPs, 9 (rs911541, rs3740066, rs11190302, rs35715207, rs3758394, rs3740058, rs3740057, rs11190315 and rs6584331) are located in a locus between *ENTPD7* and *DNMBP* recently reported by our group (26). The remaining seven, rs7909676, rs2394287, rs4459178, rs10997307, rs12258078, rs10822890 and rs713250, spanning about 38 kb, are encompassed by intron 9 of *CTNNA3*, which consists of 18 exons (Fig. 2A and C). The allelic *P*-values of these seven SNPs in the two sample sets, Exploratory and Validation, are presented in Table 2, and marker information on them is summarized in Table 3. The genotypic and allelic distributions are presented in the Supplementary Material, Table S1.

To examine the gender-specific effects of the seven *CTNNA3* SNPs on LOAD, we additionally performed joint analysis regarding gender (Table 2). For this analysis, female and male allelic contingency tables were combined for the Exploratory and Validation sets, respectively (Supplementary Material, Table S1). χ^2 tests based on the combined 2×2 allelic contingency tables and calculation of the ORs with 95% CI were carried out. In the Exploratory set comprising both genders, none of these seven SNPs showed more significant association (allelic *P*-values = 0.00005431 – 0.0235) in comparison with the Exploratory set only including females (allelic *P*-values = 0.00004614 – 0.008). The ORs exhibited a tendency to decrease; for example, for SNP rs10822890, from 1.72 to 1.55. A similar trend for both the allelic

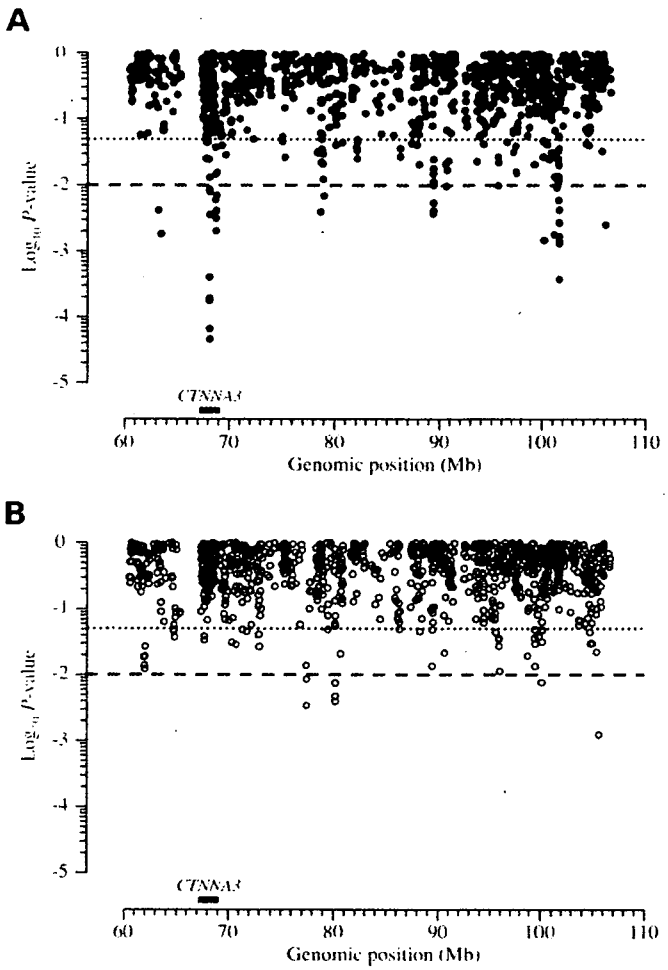

Figure 1. Allelic *P*-values of 1140 SNPs for the Exploratory set comprising female (**A**) (LOAD, 249; control, 223) or male (**B**) (LOAD, 114; control, 114) *APOE-ε3*3* subjects. Dotted and dashed lines indicate allelic *P*-values at the 0.05 and 0.01 levels, respectively. The significantly associated locus focused on in this study is indicated by the thick line, which is labeled '*CTNNA3*'. The genomic position conformed to NCBI build 35.1.

P-values and ORs of these seven SNPs was observed on Mantel–Haenszel test.

The reproducible seven SNPs on *CTNNA3* were further examined by means of stratified analysis, based on the carrier status of the *APOE-ε4* allele, with the χ^2 test (Table 4). The genotypic and allelic distributions are presented in the Supplementary Material, Table S2. We used the overall sample set, *All*, including all subjects (LOAD, 1526; controls, 1666) with all *APOE* genotypes (*2*2*, *2*3*, *2*4*, *3*3*, *3*4* and *4*4*), and two sub-sample sets, *Negative-ε4* and *Positive-ε4*, which were stratified as to the presence (*2*4*, *3*4* and *4*4*) or absence (*2*2*, *2*3* and *3*3*) of the *APOE-ε4* allele (Table 1). As shown in Table 4, in the All set, five (rs7909676, rs2394287, rs4459178, rs10822890 and rs713250) of the seven SNPs were statistically significant in females (allelic *P*-values = 0.0009719 – 0.00126). In the Negative-*ε4* set, all seven SNPs exhibited more significant association with LOAD in females (allelic *P*-values = 0.00001019 – 0.002555). No evidence was found of association with any of the seven SNPs in males in any sample set.

For joint analysis concerning gender, female and male contingency tables (2 × 2) with the allelic distributions were combined for the All, Negative-*ε4* and Positive-*ε4* sample sets, respectively (Supplementary Material, Table S2). Allelic *P*-values and ORs (95% CI) derived from the combined contingency tables were used to evaluate the gender-specific effects on LOAD (Table 4). This analysis revealed that in the All set including both genders, the ORs of significant SNPs (rs7909676, rs10822890 and rs713250) tended to be lower, compared with those in the female All set; for example, from 1.23 to 1.11 for SNP rs713250. A similar decreasing tendency for ORs of significant SNPs (rs7909676, rs2394287, rs4459178, rs10997307, rs12258078, rs10822890 and rs713250) in the Negative-*ε4* set including both genders was also observed in comparison with those in the female Negative-*ε4* set; for example, from 1.42 to 1.24 for SNP rs10822890.

Multiple logistic regression analysis, involving *APOE-ε4*, gender, age, the seven replicated SNPs on *CTNNA3* and their interactions as independent variables, was performed to assess the potential effects of these variables on the association with LOAD, using 2762 subjects [LOAD, 1313 (female, 949; male, 364); controls, 1449 (female, 877; male, 572)] (Table 5). In this analysis, the subjects used were not sub-grouped as to gender and/or carrier status of the *APOE-ε4* allele. Initially, we carried out multiple logistic regression analysis with a forward stepwise method without interaction terms to elucidate which variables explained an association with LOAD independently. Model 1 in Table 5 shows significant risk factors selected by this analysis. Expectedly, the *APOE-ε4* allele, gender and age, which are well-known risk factors for LOAD, had significant effects on the LOAD risk. Among the seven associated SNPs, SNP rs713250 was chosen as representative and selectively entered in this model [for genotype CC: OR (95% CI), 1.36 (1.08–1.71); *P*-value = 0.009]. Following this primary analysis, we further assessed second-order interaction terms created by the four significant risk factors including the SNP rs713250 (Model 2 in Table 5). Six interactions were tested by means of a forward stepwise method in addition to *APOE-ε4*, gender, age and the SNP rs713250. It was demonstrated that the SNP rs713250 exhibited significant interaction with the female gender in a dose-dependent manner as to the allele C [TC_female, OR (95% CI) = 1.68 (1.12–2.54); CC_female, OR (95% CI) = 2.57 (1.59–4.17)].

Linkage disequilibrium and case–control haplotype analyses

To reveal genetic relationship between each significant SNP on *CTNNA3*, linkage disequilibrium (LD) and haplotype estimation analyses were performed. For these analyses, we used four sample sets (All as the overall sample set, and Negative-*ε4*, Positive-*ε4* and *ε3*3* as sub-sample sets) after being sub-grouped as to gender (Table 1). From the Japanese HapMap genotype data (JPT), these SNPs were found to be encompassed by a highly structured LD block extending about 80 kb from 68.10 to 68.18 Mb (Fig. 2B). They were in strong LD: the robust LD block structures did not differ between females and males or between LOAD and controls in any sample set (Supplementary Material, Fig. S1).

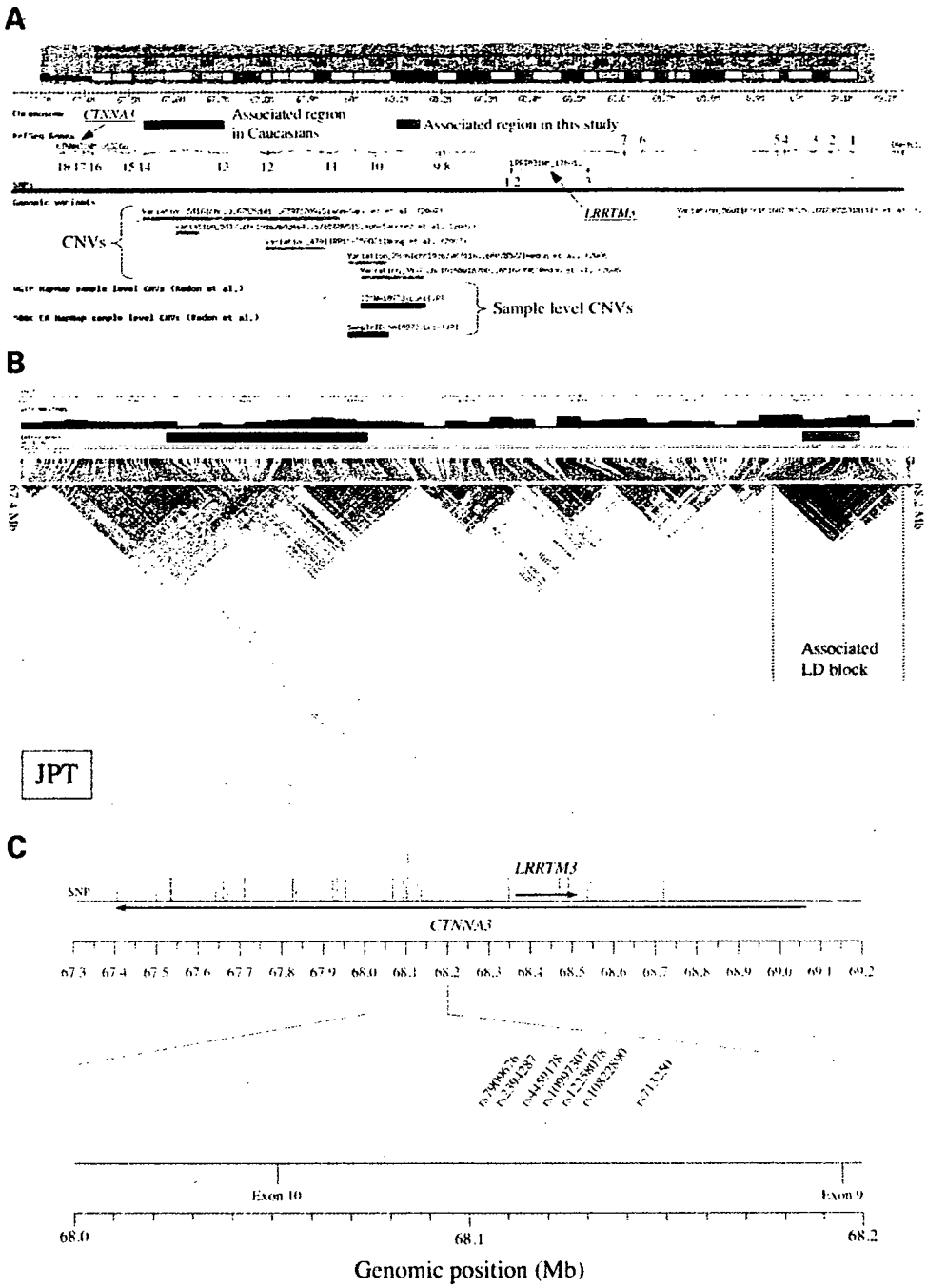

Figure 2. Genomic position and LD block structure of an associated locus within *CTNNA3*. (**A**) Genomic region including *CTNNA3* from web site Database of Genomic Variation (http://projects.tcag.ca/variation/). Boxes filled in green and black, also used in Fig. 2B, represent the associated genomic regions identified here and in studies on Caucasians (32,35,37), respectively. Each exon of *CTNNA3* and *LRRTM3* is numbered; CNV, copy number variation. (**B**) Overview of the LD pattern between 67.4 and 68.2 Mb in Japanese. HapMap genotype data (1768 SNPs) on 45 unrelated Japanese in Tokyo (JPT) were used as calculation of LD measures, D'. (**C**) Physical positions of the seven replicated SNPs. Vertical lines indicate the SNPs used in this study: significantly associated SNPs are indicated by the long labeled vertical lines. Horizontal arrows within open boxes indicate the transcription orientations of individual genes. The mapping position of each SNP is according to dbSNP build 125 on NCBI build 35.1.

Four haplotypes were estimated in each LD block consisting of the seven SNPs: three major haplotypes (frequency >0.1), [H1]C-A-T-T-T-A-T, [H2]A-G-C-C-G-G-C and [H3]A-G-C-T-T-G-C, and one minor haplotype, [H4]C-A-T-T-T-A-C (Table 6). H1 exhibited the highest frequency (range 0.4363–0.5356) and H4 the lowest (range 0.0084–0.031). Haplotypes H1, H2 and H3 were always estimated with the expectation-maximization (EM) algorithm in the four sample sets examined. Haplotype H4 was not inferred in either Negative-*ε4* or *ε3*3* consisting of male subjects.

Table 2. Statistics for seven reproducible SNPs found on two-step screening involving *APOE-ε3*3*

Sample set	Exploratory		Validation		Exploratory + Validation[a]	
Female						
Number of subjects						
LOAD	249		242		491	
Control	223		213		436	
dbSNP	Allelic *P*-value	OR (95% CI)	Allelic *P*-value	OR (95% CI)	Allelic *P*-value	OR (95% CI)
rs7909676	***0.0004042***	1.61 (1.23–2.09)	***0.0132***	1.40 (1.07–1.82)	***0.00002087***	1.50 (1.24–1.81)
rs2394287	***0.0001782***	1.64 (1.27–2.13)	***0.0427***	1.31 (1.01–1.71)	***0.00004311***	1.47 (1.22–1.77)
rs4459178	***0.0001939***	1.64 (1.26–2.13)	***0.0296***	1.34 (1.03–1.75)	***0.00002885***	1.49 (1.23–1.79)
rs10997307	***0.008686***	1.45 (1.10–1.91)	***0.0372***	1.34 (1.02–1.76)	***0.0008809***	1.39 (1.15–1.69)
rs12258078	***0.008***	1.44 (1.10–1.89)	***0.0352***	1.34 (1.02–1.76)	***0.0007658***	1.39 (1.15–1.68)
rs10822890	***0.00004614***	1.72 (1.32–2.23)	***0.0266***	1.35 (1.04–1.75)	***0.000008277***	1.52 (1.27–1.83)
rs713250	***0.00006663***	1.69 (1.31–2.20)	***0.0162***	1.38 (1.06–1.80)	***0.000005945***	1.53 (1.27–1.84)
Male						
Number of subjects						
LOAD	114		94		208	
Control	114		159		273	
dbSNP	Allelic *P*-value	OR (95% CI)	Allelic *P*-value	OR (95% CI)	Allelic *P*-value	OR (95% CI)
rs7909676	0.2961	1.22 (0.84–1.77)	0.1933	0.78 (0.54–1.13)	0.8507	0.98 (0.75–1.27)
rs2394287	0.3418	1.20 (0.83–1.74)	***0.0183***	0.64 (0.44–0.93)	0.3125	0.87 (0.67–1.14)
rs4459178	0.3456	1.20 (0.82–1.74)	***0.0209***	0.65 (0.45–0.94)	0.3231	0.88 (0.67–1.14)
rs10997307	0.9594	1.20 (0.69–1.48)	0.2477	0.79 (0.54–1.17)	0.4350	0.90 (0.68–1.18)
rs12258078	0.8457	1.01 (0.71–1.52)	0.1901	0.77 (0.52–1.14)	0.4308	0.90 (0.68–1.18)
rs10822890	0.2235	1.26 (0.87–1.83)	***0.0237***	0.65 (0.45–0.95)	0.4534	0.91 (0.70–1.18)
rs713250	0.2588	1.24 (0.85–1.79)	0.0578	0.70 (0.49–1.01)	0.5761	0.93 (0.72–1.20)
Female + male						
Number of subjects						
LOAD	363		336		699	
Control	337		372		709	
dbSNP	Allelic *P*-value	OR (95% CI)	Allelic *P*-value	OR (95% CI)	Allelic *P*-value	OR (95% CI)
rs7909676	***0.0004364***	1.47 (1.19–1.82)	0.1668	1.16 (0.94–1.44)	***0.0005443***	1.30 (1.12–1.52)
rs2394287	***0.0002861***	1.48 (1.20–1.84)	0.6336	1.05 (0.85–1.30)	***0.003812***	1.25 (1.07–1.45)
rs4459178	***0.0003147***	1.48 (1.20–1.84)	0.5868	1.06 (0.86–1.31)	***0.003417***	1.25 (1.08–1.46)
rs10997307	***0.0321***	1.28 (1.02–1.60)	0.2511	1.14 (0.91–1.42)	***0.02028***	1.20 (1.03–1.41)
rs12258078	***0.0235***	1.29 (1.03–1.61)	0.2757	1.13 (0.91–1.40)	***0.01778***	1.21 (1.03–1.41)
rs10822890	***0.00005431***	1.55 (1.25–1.92)	0.4934	1.08 (0.87–1.33)	***0.0008589***	1.29 (1.11–1.50)
rs713250	***0.00008381***	1.53 (1.24–1.89)	0.2786	1.12 (0.91–1.39)	***0.0003985***	1.31 (1.13–1.52)

Allelic *P*-values and ORs, with 95% CI in parentheses, are indicated. Boldface indicates statistically significant results (allelic *P*-value <0.05). The genotypic and allelic distributions are shown in the Supplementary Material, Table S1.
[a]Computed by the method of Mantel and Haenszel.

Table 3. Summary of seven associated SNPs within intron 9 of *CTNNA3*

dbSNP	Genomic position (bp)[a]	Alleles[b]	Exploratory				Validation			
			GSR	Frequency[c]	HWE[d]		GSR	Frequency[e]	HWE[f]	
					LOAD	Control			LOAD	Control
rs7909676	68 104 803	C/A	96.43	0.507/0.493	0.3377	0.8206	96.75	0.506/0.494	0.6566	0.9161
rs2394287	68 105 668	A/G	97.57	0.521/0.480	0.5934	0.5760	97.88	0.517/0.483	0.741	1.0000
rs4459178	68 114 303	T/C	96.71	0.512/0.488	0.9137	0.5778	96.47	0.514/0.486	0.5784	0.9159
rs10997307	68 119 438	T/C	95.00	0.633/0.367	0.9107	0.6173	97.74	0.640/0.360	1.0000	0.1316
rs12258078	68 125 734	T/G	99.29	0.641/0.359	0.9116	0.6219	99.01	0.641/0.359	1.0000	0.1686
rs10822890	68 127 819	A/G	97.71	0.516/0.484	0.5208	0.5757	97.60	0.515/0.486	0.5055	1.0000
rs713250	68 143 405	C/T	98.43	0.501/0.499	0.5211	0.6579	98.45	0.503/0.497	0.7415	0.9170

GSR, genotyping success rate.
[a]Based on dbSNP build 125 on NCBI build 35.1.
[b]Nucleotides of the major allele/minor allele.
[c]The major allele/minor allele frequency, calculated using genotype data obtained for 363 LOAD patients and 337 controls with *APOE-ε3*3* in the Exploratory set.
[d]*P*-values were calculated with exact tests of HWE using both 363 LOAD patients and 337 controls with *APOE-ε3*3* in the Exploratory set.
[e]The major allele/minor allele frequency, calculated using genotype data obtained for 336 LOAD patients and 372 controls with *APOE-ε3*3* in the Validation set.
[f]*P*-values were calculated with exact tests of HWE using both 336 LOAD patients and 372 controls *APOE-ε3*3* in the Validation set.

Table 4. Allelic association of seven associated SNPs, encompassed by intron 9 of *CTNNA3*, in the overall sample set, All, and two sub-sample sets, Negative-*ε4* and Positive-*ε4*, stratified as to the presence or absence of the *APOE-ε4* allele

Gender	Female		Male		Female + male	
Sample set	All[a]					
Number of subjects						
LOAD	1103		423		1526	
Control	998		668		1666	
dbSNP	Allelic *P*-value	OR (95% CI)	Allelic *P*-value	OR (95% CI)	Allelic *P*-value	OR (95% CI)
rs7909676	***0.001646***	1.22 (1.08–1.38)	0.2558	0.90 (0.76–1.08)	***0.0472***	1.11 (1.00–1.22)
rs2394287	***0.001696***	1.22 (1.08–1.38)	0.1906	0.89 (0.75–1.06)	0.0512	1.10 (1.00–1.22)
rs4459178	***0.002843***	1.21 (1.07–1.37)	0.2085	0.89 (0.75–1.07)	0.0681	1.10 (0.99–1.21)
rs10997307	0.2316	1.08 (0.95–1.23)	0.4329	0.93 (0.77–1.12)	0.517	1.03 (0.93–1.15)
rs12258078	0.2307	1.08 (0.95–1.23)	0.5439	0.94 (0.79–1.13)	0.4422	1.04 (0.94–1.16)
rs10822890	***0.00126***	1.22 (1.08–1.38)	0.2137	0.89 (0.75–1.07)	***0.0402***	1.11 (1.00–1.23)
rs713250	***0.0009719***	1.23 (1.09–1.39)	0.1358	0.88 (0.73–1.04)	***0.0439***	1.11 (1.00–1.22)
Sample set	Negative-*ε4*[b]					
Number of subjects						
LOAD	522		227		749	
Control	827		551		1378	
dbSNP	Allelic *P*-value	OR (95% CI)	Allelic *P*-value	OR (95% CI)	Allelic *P*-value	OR (95% CI)
rs7909676	***0.00001471***	1.42 (1.21–1.66)	0.6951	0.96 (0.76–1.20)	***0.0008525***	1.24 (1.09–1.41)
rs2394287	***0.00005357***	1.38 (1.18–1.62)	0.4346	0.91 (0.73–1.14)	***0.003869***	1.21 (1.06–1.37)
rs4459178	***0.00005308***	1.39 (1.18–1.62)	0.4728	0.92 (0.74–1.15)	***0.003415***	1.21 (1.07–1.38)
rs10997307	***0.002555***	1.28 (1.09–1.51)	0.8393	0.98 (0.77–1.23)	***0.0163***	1.18 (1.03–1.34)
rs12258078	***0.001978***	1.29 (1.10–1.52)	0.8693	0.98 (0.78–1.24)	***0.0129***	1.18 (1.04–1.35)
rs10822890	***0.00001019***	1.42 (1.22–1.67)	0.5198	0.93 (0.74–1.16)	***0.001046***	1.24 (1.09–1.41)
rs713250	***0.00001576***	1.41 (1.21–1.65)	0.5154	0.93 (0.74–1.16)	***0.001162***	1.24 (1.09–1.40)
Sample set	Positive-*ε4*[c]					
Number of subjects						
LOAD	581		196		777	
Control	171		117		288	
dbSNP	Allelic *P*-value	OR (95% CI)	Allelic *P*-value	OR (95% CI)	Allelic *P*-value	OR (95% CI)
rs7909676	0.8115	0.97 (0.76–1.24)	0.1917	0.80 (0.58–1.12)	0.3764	0.92 (0.75–1.11)
rs2394287	0.8995	0.98 (0.77–1.26)	0.4275	0.87 (0.63–1.22)	0.7096	0.96 (0.79–1.17)
rs4459178	0.7375	0.96 (0.75–1.23)	0.2844	0.84 (0.60–1.16)	0.438	0.93 (0.76–1.12)
rs10997307	***0.0409***	0.77 (0.60–0.99)	0.4491	0.88 (0.62–1.24)	0.0528	0.82 (0.67–1.00)
rs12258078	***0.0306***	0.76 (0.59–0.97)	0.6752	0.93 (0.66–1.31)	0.0727	0.83 (0.68–1.02)
rs10822890	0.582	0.93 (0.73–1.19)	0.2816	0.84 (0.60–1.16)	0.3617	0.91 (0.75–1.11)
rs713250	0.9234	0.99 (0.77–1.26)	0.0784	0.74 (0.54–1.03)	0.3245	0.91 (0.75–1.10)

Allelic *P*-values and ORs, with 95% CI in parentheses, are indicated. Boldface indicates statistically significant results (allelic *P*-values <0.05). The genotypic and allelic distributions are shown in the Supplementary Material, Table S2.

[a]All *APOE* genotypes (*APOE-ε2**2, *2*3*, *2*4*, *3*3*, *3*4* and *4*4*) comprising those of 1526 LOAD patients (female, 1103; male, 423) and 1666 controls (female, 998; male, 668).

[b]Non-carriers of the *APOE-ε4* allele (*2*2*, *2*3* and *3*3*) comprising 749 LOAD patients (female, 522; control, 227) and 1378 controls (female, 827; male, 551).

[c]Carriers of the *APOE-ε4* allele (*2*4*, *3*4* and *4*4*) comprising 777 LOAD patients (female, 581; male, 196) and 288 controls (female, 171; male, 117).

Because multiple SNPs may increase the risk of LOAD in combination, we carried out a case–control haplotype analysis (Table 6). In the All set, haplotypes H1 (permutation *P*-value = 0.0029) and H3 (permutation *P*-value = 0.0043) exhibited significant association in females. In both the Negative-*ε4* and *ε3*3* sets, haplotypes H1, H2 and H3 exhibited significance in females (permutation *P*-value H1 < H2 < H3). In the All, Negative-*ε4* and *ε3*3* sets, the frequency of haplotype H1 was decreased in LOAD, suggesting it is a protective haplotype for LOAD. On the other hand, haplotypes H2 and H3 were increased in LOAD, implying that they are risk haplotypes for LOAD. In males, each haplotype showed no significant difference in any sample set.

Of the four sample sets of females, three showed significant association in global tests: All (global permutation *P*-value = 0.0006), Negative-*ε4* (global permutation *P*-value = 0.0008), and *ε3*3* (global permutation *P*-value = 0.001). We did not detect significance in any haplotype in the female sub-sample set Positive-*ε4* (global permutation *P*-value = 0.3323).

Relationship between the Aβ40/42 ratio and genetic variation on *CTNNA3*

The levels of plasma Aβ40 and Aβ42 and their ratio (Aβ40/42) were compared between LOAD patients ($N = 456$) and control subjects ($N = 147$) within different gender groups (Fig. 3A–C). The Mann–Whitney *U*-test was adopted as a non-parametric method for this analysis. In both the female and male groups, the Aβ40 levels (Fig. 3A) and Aβ40/42 ratio (Fig. 3C) were significantly higher in LOAD in comparison with those in controls. The Aβ42 levels were significantly lower in LOAD compared with those in controls (Fig. 3B).

Table 5. Multiple logistic regression analysis

Variables[a]	Category	OR (95% CI)
Model 1		
APOE	*ε4* (−) (Ref)	1.00
	ε4 (+)	**5.00 (4.20–5.96)***
Gender	Male (Ref)	1.00
	Female	**1.64 (1.38–1.94)***
SNP rs713250[b]	TT (Ref)	1.00
	TC	1.13 (0.92–1.37)
	CC	**1.36 (1.08–1.71)****
Age	—	**1.01 (1.00–1.02)*****
Model 2		
APOE	*ε4* (−) (Ref)	1.00
	ε4 (+)	**5.74 (3.62–9.10)***
Gender	Male (Ref)	1.00
	Female	0.88 (0.62–1.26)
SNP rs713250[b]	TT (Ref)	1.00
	TC	0.81 (0.58–1.12)
	CC	0.75 (0.51–1.10)
Age	–	**1.02 (1.01–1.03)****
SNP rs713250_gender[b]	Others (Ref)	1.00
	TC_Female	**1.68 (1.12–2.54)*****
	CC_Female	**2.57 (1.59–4.17)***
Age_*APOE*	Age_*ε4* (−) (Ref)	1.00
	Age_*ε4* (+)	**0.97 (0.95–1.00)*****
Gender_*APOE*	Others (Ref)	1.00
	Female_*ε4* (+)	**1.49 (1.03–2.15)*****

Ref, reference.
*P-value <0.001; **P-value <0.01; ***P-value <0.05.
[a]'_' signifies the interaction between variables.
[b]Global P-value <0.05.

To determine whether or not the difference in the Aβ40/42 ratio between LOAD and the controls is due to the SNPs identified here, two-way ANOVA was performed across diagnosis (LOAD and control) and three genotypic groups (major homozygotes, heterozygotes and minor homozygotes) within different gender and their combined groups (Fig. 3D–F). SNP rs713250 was used as a representative of the seven associated SNPs because it showed the most significant association with LOAD on Mantel–Haenszel test (allelic $P\text{-value}_{MH\text{-}F} = 0.000005945$), as shown in Table 2. The log-transformed Aβ40/42 ratio values [$\log_2$(Aβ40/42 ratio + 1)] were used in this analysis. Before two-way ANOVA, the Kolmogorov–Smirnov (KS) normality test and Bartlett's test for equal variances were performed for the each dataset as to gender. Almost every sub-group examined passed the KS normality test. Both the female–male (Fig. 3D) and female (Fig. 3E) groups passed the Bartlett's test, but not the male group (Fig. 3F, $P = 0.01178$). Through two-way ANOVA, a significant effect of diagnosis was observed for every group (P-values <0.0001). However, we did not detect any genotype-dependent effect of this SNP on the Aβ40/42 ratio, and no interaction between the SNP, Aβ40/42 ratio and diagnosis.

DISCUSSION

In this study, we extended our previous work on chromosome 10q (26), and thoroughly reanalyzed the genotype data for 1140 SNPs in order to discover gender-related genetic loci for LOAD. In a single SNP-based case control study, we found seven SNPs on *CTNNA3* showing genetic association with LOAD in females with the *APOE-ε3*3* genotype or without the *APOE-ε4* allele. Furthermore, multiple logistic regression analysis revealed that one (SNP rs713250) of these seven SNPs directly interacted with the female gender, but not with the male gender, and did not show any interaction with the *APOE-ε4* allele at all. These are the first findings constituting evidence that *CTNNA3* may affect the development of sporadic LOAD through a novel female-specific mechanism independent of the *APOE-ε4* allele. We consider the genetic association identified here to reflect one single signal. The reasons are: (1) the seven significant SNPs span only ~38 kb and are clustered in intron 9 of *CTNNA3* (Fig. 2A and C), which suggests a multiple-hit genomic region of SNPs associated with LOAD; (2) solid linkage disequilibrium was observed between all of these seven SNPs ($D' > 0.9$) (Supplementary Material, Fig. S1); and (3) the associated region was encompassed by a tight structured LD block extending ~80 kb (Fig. 2B).

Janssens *et al.* (29,30) cloned full-length *CTNNA3* cDNA as a novel member of the α-catenin gene family and determined its genomic structure. *CTNNA3* contains 18 exons and spans ~1.78 Mb (67.35–69.13 Mb), being the longest of all genes located on chromosome 10. The chromosomal location of *CTNNA3* is 10q21 (30), which includes the suggestive linkage region between microsatellite markers D10S1227 (57.20 Mb) and D10S1211 (66.39 Mb) in LOAD (24). Ertekin-Taner *et al.* (23) found a linkage with a maximum LOD score of 3.93 at 81 cM close to D10S1225 (64.43 Mb) using the plasma Aβ42 level as a surrogate trait in a set of LOAD families, and the same chromosomal region was identified by Myers *et al.* (24) by means of genome-wide screening of sibling pairs with LOAD. To date, there have been six papers on the genetic association of *CTNNA3* with LOAD (32–37). In the first report (32), it was demonstrated that two SNPs located in intron 13 of *CTNNA3* are associated with familial LOAD with high levels of plasma Aβ42, which was used as an intermediate phenotype related to AD. These intronic SNPs, spanning 423 bp, are rs12357560 and rs7070570: the former lies 1174 bp upstream, and the latter 1597 bp downstream from exon 14, respectively. They are in strong LD: $D'=1$ in all four populations, CEU, CHB, JPT and YRI, used in the HapMap project (38). A genotype-dependent correlation between SNP rs7070570 and the plasma Aβ42 level has also been detected: the major homozygote (TT) is associated with the highest level of Aβ42, the heterozygote (TC) with an intermediate level and the minor homozygote (CC) with the lowest level (32). Martin *et al.* (34), found that SNP rs7074454 located in intron 13 of *CTNNA3*, lying 355 bp upstream from SNP rs7070570, was significantly associated with both familial and sporadic cases of LOAD. Non-synonymous SNP rs4548513 (AGC → AAC, Ser596Asn) located in exon 13 of *CTNNA3*, lying 175 721 bp upstream from SNP rs7070570, has been shown to be associated with familial AD (37). All of these four SNPs, rs7070570, rs12357560, rs7074454 and rs4548513, lie in a genomic region extending from exons 13 to 14 (Fig. 2A), which has been shown to be located within a large LD block spanning around 310 kb (67.43–67.74 Mb)

Table 6. Case–control haplotype analysis

Sample set	Gender	Number of subjects		Haplotype[a]	Frequency		Number of estimated alleles		Permutation *P*-value (10 000)	OR (95% CI)
		LOAD	Control		LOAD	Control	LOAD	Control		
All	Female	1103	998	**[H1]C-A-T-T-T-A-T**	0.4717	0.5174	1041	1033	**0.0029**	0.83 (0.74–0.94)
				[H2]A-G-C-C-G-G-C	0.3592	0.3375	792	674	0.1538	1.10 (0.97–1.25)
				[H3]A-G-C-T-T-G-C	0.1406	0.1110	310	222	**0.0043**	1.31 (1.09–1.57)
				[H4]C-A-T-T-T-A-C	0.0196	0.0169	43	34	0.5632	1.15 (0.73–1.81)
				Others[b]	0.0089	0.0172	20	33	–	–
				Sum	1.0000	1.0000	2206	1996		–
				Global	–	–	–	–	**0.0006**	–
	Male	423	668	[H1]C-A-T-T-T-A-T	0.5293	0.4973	448	664	0.145	1.14 (0.96–1.35)
				[H2]A-G-C-C-G-G-C	0.3344	0.3415	283	456	0.7739	0.97 (0.81–1.16)
				[H3]A-G-C-T-T-G-C	0.1179	0.1314	100	176	0.3927	0.88 (0.68–1.15)
				[H4]C-A-T-T-T-A-C	0.0084	0.0131	7	18	0.3117	0.61 (0.25–1.47)
				Others[b]	0.01	0.0167	8	22		
				Sum	1.0000	1.0000	846	1336		
				Global					0.2273	
Negative-*ε4*	Female	522	827	**[H1]C-A-T-T-T-A-T**	0.4430	0.5228	462	865	**< 0.0001**	0.72 (0.62–0.85)
				[H2]A-G-C-C-G-G-C	0.3888	0.3273	406	541	**0.0008**	1.31 (1.11–1.54)
				[H3]A-G-C-T-T-G-C	0.1418	0.1132	148	187	**0.0323**	1.30 (1.02–1.63)
				[H4]C-A-T-T-T-A-C	0.0206	0.0185	22	31	0.6661	1.13 (0.65–1.96)
				Others[b]	0.0058	0.0182	6	30		
				Sum	1.0000	1.0000	1044	1654		
				Global					**0.0008**	
	Male	227	551	[H1]C-A-T-T-T-A-T	0.5240	0.5039	238	556	0.5078	1.08 (0.87–1.35)
				[H2]A-G-C-C-G-G-C	0.3479	0.3456	158	381	0.9532	1.01 (0.80–1.27)
				[H3]A-G-C-T-T-G-C	0.1167	0.1289	53	142	0.5618	0.89 (0.64–1.25)
				Others[b]	0.0114	0.0216	5	23	–	–
				Sum	1.0000	1.0000	454	1102		
				Global					0.7917	
*ε3*3*	Female	491	748	**[H1]C-A-T-T-T-A-T**	0.4363	0.5179	428	775	**0.0002**	0.72 (0.61–0.85)
				[H2]A-G-C-C-G-G-C	0.3919	0.3305	385	494	**0.0019**	1.31 (1.11–1.55)
				[H3]A-G-C-T-T-G-C	0.1436	0.1151	141	172	**0.0405**	1.29 (1.02–1.64)
				[H4]C-A-T-T-T-A-C	0.0219	0.0178	22	27	0.4617	1.25 (0.71–2.20)
				Others[b]	0.0063	0.0187	6	28		
				Sum	1.0000	1.0000	982	1496		
				Global					**0.001**	
	Male	208	495	[H1]C-A-T-T-T-A-T	0.5214	0.4995	217	491	0.383	1.11 (0.88–1.39)
				[H2]A-G-C-C-G-G-C	0.3459	0.3525	144	349	0.8585	0.97 (0.76–1.24)
				[H3]A-G-C-T-T-G-C	0.1202	0.1300	50	129	0.6659	0.91 (0.64–1.29)
				Others[b]	0.0125	0.0220	5	21		
				Sum	1.0000	1.0000	416	990	–	–
				Global	–	–	–	–	0.8879	
Positive-*ε4*	Female	581	171	[H1]C-A-T-T-T-A-T	0.4976	0.4907	577	168	0.9006	1.02 (0.80–1.30)
				[H2]A-G-C-C-G-G-C	0.3327	0.3870	387	132	0.0799	0.79 (0.62–1.02)
				[H3]A-G-C-T-T-G-C	0.1396	0.1009	162	35	0.0797	1.42 (0.96–2.09)
				[H4]C-A-T-T-T-A-C	0.0187	0.09	22	3	0.2313	2.18 (0.65–7.33)
				Others[b]	0.0114	0.0124	14	4		
				Sum	1.0000	1.0000	1162	342	–	–
				Global	–	–	–	–	0.3323	
	Male	196	117	[H1]C-A-T-T-T-A-T	0.5356	0.4638	210	109	0.0961	1.32 (0.96–1.83)
				[H2]A-G-C-C-G-G-C	0.3188	0.3238	125	76	0.934	0.97 (0.69–1.38)
				[H3]A-G-C-T-T-G-C	0.1193	0.1459	47	34	0.3988	0.80 (0.50–1.29)
				[H4]C-A-T-T-T-A-C	0.0129	0.0310	5	7	0.1429	0.42 (0.13–1.34)
				Others[b]	0.0134	0.0355	5	8		
				Sum	1.0000	1.0000	392	234		
				Global					0.0728	

Statistically significant haplotypes and permutation *P*-values are highlighted in bold.
[a]The SNP order, from left to right, is as follows: rs7909676, rs2394287, rs4459178, rs10997307, rs12258078, rs10822890 and rs713250.
[b]Haplotypes with frequencies <0.01 in both LOAD and control subjects.

in CEU subjects (37) (Supplementary Material, Fig. S2). They have a tendency to exhibit selective association with familial rather than sporadic LOAD (32,35,37). Therefore, it is likely that the large LD block region contributes to a specific form of familial LOAD in Caucasians. We also assessed these four SNPs and SNPs neighboring them in our Japanese sporadic LOAD subjects, however, none of these SNPs exhibited significant association (data not shown). In the genomic

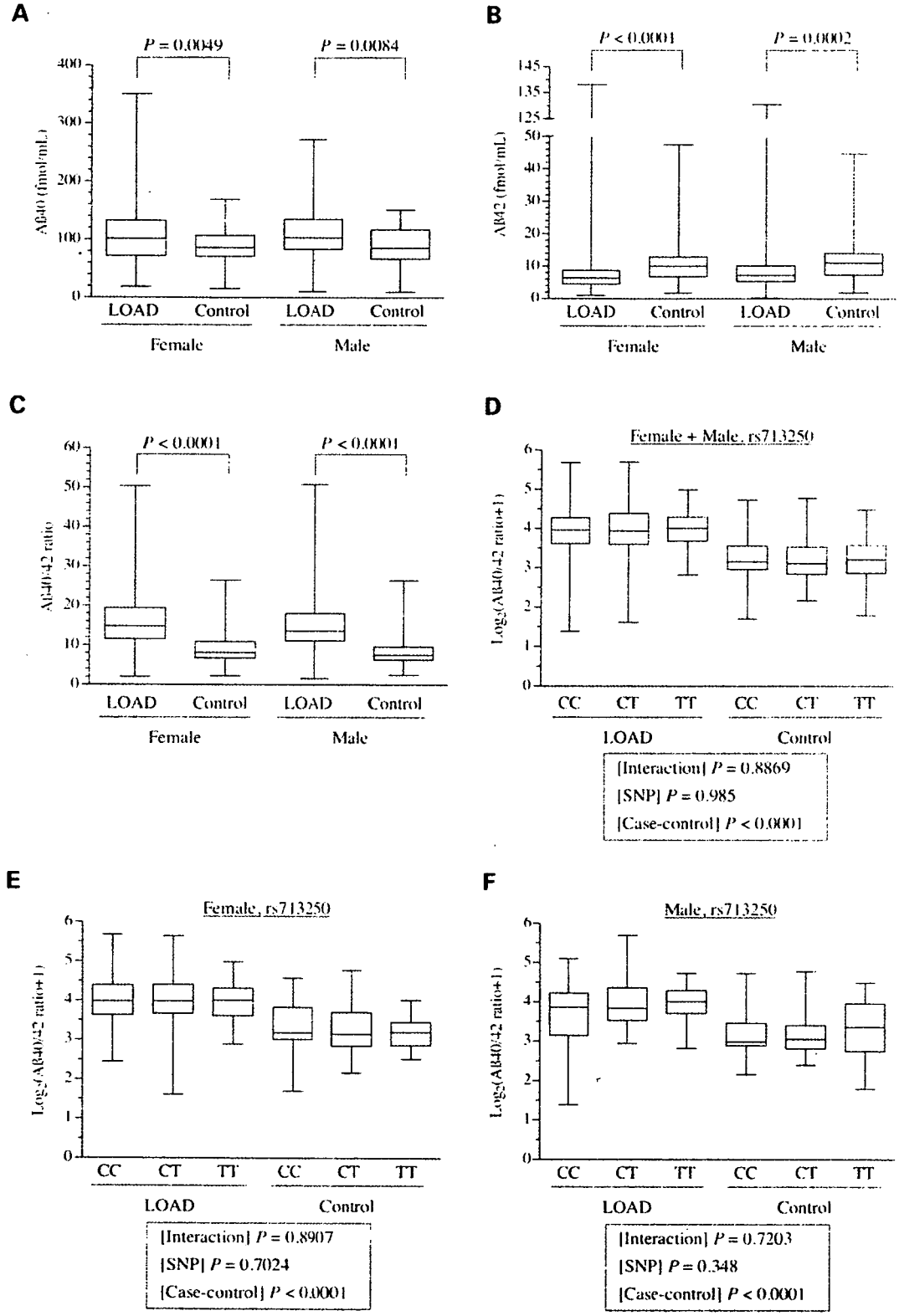

Figure 3. Comparison of the plasma levels of Aβ40 and Aβ42, and the Aβ40/42 ratio. The differences in the relative amounts of Aβ40 (**A**) and Aβ42 (**B**), and the Aβ40/42 ratio (**C**) were compared between LOAD patients and controls by means of Mann–Whitney's *U*-test within different gender groups. (**D**, **E**, **F**) Correlation between the Aβ40/42 ratio, an associated SNP on *CTNNA3*, and the diagnosis (LOAD or control). Using log-transformed Aβ40/42 ratio values, two-way ANOVA tests were performed after Bartlett's test for the homogeneity of variances and the KS normality test. The results for SNP rs713250 are presented here as being representative of the seven associated SNPs identified in this study. The horizontal line inside each box denotes the median value. The box extends from the 25th and 75th percentiles. The error bars extend down to the lowest value and up to the highest. Genotypes CC, CT and TT represent major-allele homozygotes, heterozygotes and minor-allele homozygotes, respectively.

region including the four SNPs, different LD block structures were observed in Japanese and CEPH subjects (Fig. 2B and Supplementary Material, Fig. S2). As one of the reasons why reproducible association could not be detected for these four SNPs, we mainly consider that an ethnic difference may exist.

High-level gene expression of *CTNNA3* is detected predominantly in heart and testis, and low-level expression in several tissues including brain (29). Coimmunoprecipitation analysis revealed that CTNNA3 binds directly to β-catenin in both a human cell line transfected with *CTNNA3* cDNA, and heart and testis tissue extracts of mouse (30). β-Catenin forms a complex with presenilin 1 (PSEN1) (31,39,40), mutations of which cause familial cases of early-onset AD (EOAD) [Alzheimer Disease & Frontotemporal Dementia Mutation Database (AD&FTDMDB), http://www.molgen.ua.ac.be/ADMutations/]. The expression level of β-catenin is reduced in the brains of EOAD patients with *PSEN1* mutations (31). Intracellular trafficking of β-catenin is affected in human cells bearing *PSEN1* mutations (41), resulting in sustained loss of Wnt/β-catenin signal transduction, which is probably followed by the onset and development of AD (42,43). Although, at present, there is no direct evidence suggesting that CTNNA3 interacts with PSEN1, it is assumed that their genetic polymorphisms or combinations in *CTNNA3* may have a negative influence on the Wnt/β-catenin signaling pathway, leading to potential involvement in the pathogenesis of AD. In this study, it was clarified that seven intronic SNPs on *CTNNA3* were significantly and reproducibly associated with sporadic female cases of LOAD without the *APOE-ε4* allele. Intronic variants are considered to have the potential to directly affect gene-expression levels in some cases (44); therefore, we performed quantitative real-time RT–PCR analysis of *CTNNA3* using the postmortem brains of 19 neuropathologically-confirmed LOAD cases and 22 control ones. Two-way ANOVA revealed that there was no statistically significant interaction between the *CTNNA3* expression level, the associated SNPs identified here and the diagnosis (data not shown). Additionally, although a genotype-dependent transition effect on the plasma Aβ42 level was observed for intronic SNP rs7070570 by Ertekin-Taner *et al.* (32), it was found that none of these SNPs influence the plasma levels of Aβ peptides (Fig. 3D–F).

However, interestingly, by means of a search of a public genome database, the Database of Genomic Variants (http://projects.tcag.ca/variation/), we discovered that there is copy number variation (CNV) (45) in the genomic region comprising the seven associated SNPs on *CTNNA3*: variation ID 3807 at Locus 2128, which was detected in a Japanese subject (ID, NA18973) (Fig. 2A). CNV, i.e. deletion, insertion and duplication with >1 kb in length of the genomic sequence (46), rather than SNP could cause phenotypic diversity and complex diseases in humans by altering the gene dose or disrupting the coding or regulatory sequences of genes, and may account for the LOAD susceptibility. Regarding our LOAD subjects, we did not examine the presence or absence of CNV within *CTNNA3*. Therefore, in a further study, it is very important to determine whether or not CNV in *CTNNA3* is associated with LOAD.

Recently, in LOAD families, notable evidence was obtained suggesting a maternal parent-of-origin effect on chromosome 10q between microsatellite markers D10S1233 (44.05 Mb) and D10S1225 (64.43 Mb) with a non-parametric LOD score >1.0: the highest LOD score of 3.73 was seen for microsatellite marker D10S1221 (57.20 Mb) (27,28). Moreover, it was found that *CTNNA3* is subject to genomic imprinting with cell-type specificity in placental tissues: biallelic and monoallelic (maternal-allele) expression is observed in extravillus and villus trophoblasts, respectively (47). Mouse *Ctnna3* (Clone ID 4933408A16 on FANTOM2), orthologous to human *CTNNA3*, has been deposited as a maternal imprinting gene on chromosome 10 in the Expression-based Imprint Candidate Organizer DataBase (48; EICO DB, http://fantom2.gsc.riken.jp/EICODB/imprinting/), provided by RIKEN (Japan). These findings led us to examine whether or not *CTNNA3* shows allele-specific expression caused by a molecular mechanism such as genomic imprinting in the brain. We conducted real-time RT–PCR analysis with allele-specific amplification using postmortem human brains heterozygous for non-synonymous SNP rs4548513 in exon 13 [LOAD, 7 (female:male = 3:4); control, 8 (female:male = 3:5)]. Unexpectedly, biallelic expression was detected in brain tissues, and there was no significant difference between LOAD patients and control subjects in the expression level of *CTNNA3* (data not shown). Since as in placental tissues, as described above, it is possible that cell-type dependent imprinting for *CTNNA3* may occur in the brain, further expression analysis should be carefully carried out using homogeneous populations of specific cells from brain tissues. Now genome-wide prediction and the discovery of imprinted genes have progressed (49,50), and 600 (2.5%) of 23 788 annotated autosomal genes have been found to be potentially imprinted in the mouse genome by computational estimation: 384 (64%) of these candidate-imprinted genes show maternal-allele expression (50). It is expected that failure of imprinted gene expression in the human brain may lead to cognition and behavior defects such as Alzheimer's disease, schizophrenia, the bipolar affective disorder and epilepsy (51–53). Therefore, it is important and interesting to actively examine imprinted genes present in the genetic linkage region of LOAD.

MATERIALS AND METHODS

Subjects

The Japanese Genetic Study Consortium for AD (JGSCAD) was organized in 2000, and blood samples were collected to survey risk genes for LOAD by means of a genome-wide association study. All individuals included in this study were Japanese. Probable AD cases met the criteria of the National Institute of Neurological and Communicative Disorders and Stroke-Alzheimer's Disease and Related Disorders. Control subjects who had no signs of dementia and lived in an unassisted manner in the local community were also recruited. Age at onset (AAO) is here defined as the age at which the family and/or individuals first noted cognitive problems during work or in daily activities. The Mini-Mental State Examination (MMSE), and Clinical Dementia Rating and/or the Function Assessment Staging were used for the evaluation of cognitive impairment: MMSE was used for almost every subject.

The basic demographics of the LOAD patients and non-demented control subjects are presented in Table 1. A total of 3192 subjects comprising 1526 LOAD patients [female, 1103 (72.3%); male, 423 (27.7%)] and 1666 controls [female, 998 (59.9%); male, 668 (40.1%)], which is referred to as overall sample set All in this study, were used to discover gender-related loci associated with LOAD on chromosome 10q: information on these subjects was also presented in our recent paper, Kuwano *et al.* (26). The mean AAO ± standard deviation (SD) in the 1526 LOAD patients was 73.5 ± 6.6 (range 60–93). The mean age at examination (AAE) ± SD of the control subjects was 73.1 ± 7.8 (range 60–96). There was no significant difference between AAO in LOAD patients and AAE in control subjects with the unpaired Student's *t*-test (*P*-value = 0.1239). The mean MMSE score in the 1526 LOAD patients was 16.5 (SD 7.0), which was significantly lower (*P*-value with unpaired Student's *t*-test <0.0001) than that in the 1666 controls (mean ± SD 28.0 ± 1.8). The numbers (frequency) of *APOE-ε2*2*, *ε2*3*, *ε2*4*, *ε3*3*, *ε3*4* and *ε4*4* in the 1526 LOAD subjects were 1 (0.07%), 49 (3.21%), 17 (1.11%), 699 (45.81%), 613 (40.17%) and 147 (9.63%), and those in the 1666 control subjects were 3 (0.18%), 132 (7.92%), 15 (0.90%), 1243 (74.61%), 256 (15.37%) and 17 (1.02%). The allelic distribution of *APOE* was significantly different between LOAD patients (*ε2*, 68; *ε3*, 2060; *ε4*, 924) and control subjects (*ε2*, 153; *ε3*, 2874; *ε4*, 305), as expected (*P*-value with χ^2 test using a 2×3 contingency table, <0.0001).

The present study was approved by the Institutional Review Board of Niigata University and by all participating institutes. Informed consent was obtained from all controls and appropriate proxies for patients, and all samples were anonymously analyzed for genotyping.

SNPs and genotyping

SNP information was obtained from five open databases: NCBI dbSNP (Build 125, http://www.ncbi.nlm.nih.gov/SNP/), UCSC Genome Bioinformatics (http://genome.ucsc.edu/), International HapMap Project (Rel#20/phaseII on NCBI Build 35.1 assembly and dbSNP Build 125, http://www.hapmap.org/index.html), Ensemble Human (Version 37 on NCBI Build 35.1, http://www.ensembl.org/Homo_sapiens/) and Celera myScience (Version R27 g on NCBI Build 35.1, http://myscience.appliedbiosystems.com/). We selected 1322 SNPs in the region from 60 to 107 Mb on chromosome 10q; mean intermarker distance ± SD, 34.9 ± 87.4 kb; 95% CI, 30.2–39.6 kb. The information on all SNPs, including rs or Celera IDs and genomic positions on NCBI build 35.1, used here was presented in detail elsewhere (26). These SNPs consisted of 29 missense mutations, 27 silent mutations, 6 SNPs in the 5′-UTR, 29 SNPs in the 3′-UTR, 921 SNPs in introns, 282 SNPs in intergenic regions and 28 SNPs in four loci shared by two different genes (*CTNNA3/LRRTM3*, *CDH23/C10orf54*, *C10orf55/PLAU* and *PGAM1/EXOSC1*). Among the 1322 SNPs, 28 SNPs could not be genotyped. To examine deviation from HWE of 1294 SNPs, exact tests (details given under Statistical analysis) were performed with both 363 LOAD patients and 337 control subjects (carrying *APOE-ε3*3* in the exploratory sample set, as shown in Table 1). We used 1140 SNPs that were shown to be actually polymorphic in the Japanese population and showed *P*-values >0.05 with the exact tests; mean intermarker distance ± SD, 40.5 ± 96.7 kb; 95% CI, 34.9–46.1 kb.

Genomic DNA was extracted from peripheral blood with a QIAamp DNA Blood Maxi Kit (Qiagen, Duseldorf, Germany) and examined fluorometrically with a PicoGreen dsDNA quantification kit (Molecular Probes, California, USA). SNP genotyping of individual samples was performed with an ABI PRISM 7900HT instrument using TaqMan technology, and TaqMan SNP Genotyping Assays were purchased from Applied Biosystems (California, USA).

Case–control study

To discover gender-related genetic loci on chromosome 10q (60–107 Mb on NCBI build 35.1), allelic association was assessed by means of the χ^2 test based on a 2×2 contingency table in comparison with allele frequencies in LOAD patients and control subjects within different gender groups. For screening, two independent sample sets, Exploratory and Validation, comprising case–control subjects with *APOE-ε3*3* were first used after being stratified as to gender (Table 1). Sample set Exploratory comprising 363 LOAD patients and 337 control subjects was genotyped (26), and SNPs showing significant association (allelic *P*-value <0.01) were then subjected to further examination using another sample set, Validation, comprising 336 LOAD patients and 372 control subjects. Multistage, including two-stage, genotyping designs for large-scale association surveys have been proved to be practically as well as theoretically effective for identifying common genetic variants that predispose to human disease (54–58). Therefore, we considered that replication in both the Exploratory and Validation sample sets implicates an association of particular SNPs with LOAD.

Subsequently, for stratified analysis we increased the number of subjects and constructed an overall sample set, All. Furthermore, to construct three sub-sample sets, overall sample set All was stratified as to the *APOE* carrier status: Negative-*ε4*, *APOE-ε 2*2*, *2*3* and *3*3*; *ε3*3*, *APOE-ε 3*3*; Positive-*ε4*, *APOE-ε 2*4*, *3*4* and *4*4* (Table 1). The sample numbers for LOAD patients and controls in All, Negative-*ε4*, *ε3*3* and Positive-*ε4* were 1526 and 1666, 749 and 1378, 699 and 1243, and 777 and 288, respectively. These four sample sets were used for the χ^2 test after being sub-grouped as to gender.

Case–control haplotype analysis with significant SNPs was also performed using the following sample sets: All, Negative-*ε4*, *ε3*3* and Positive-*ε4*. These four sample sets were used after being stratified as to gender.

Aβ40 and Aβ42 quantification

For Aβ40 and Aβ42 quantification, 603 subjects consisting of 456 LOAD patients (female, 332; male, 124) and 147 control subjects (female, 95; male, 52) were used. They are included in the All set. The sandwich enzyme-linked immunosorbent assay (59–61) was used to specifically quantify whole plasma Aβ species. The standardization, sensitivity and specificity of the method were described in a previous paper (61).

Briefly, microplates (Immunoplate I; Nunc, Rockilde, Denmark) were pre-coated with monoclonal BNT77 (IgA isotype specific for Aβ11–16) and then sequentially incubated for 24 h at 4 C (100 μl of whole plasma/well), followed by 24 h incubation at 4°C with horseradish-peroxidase-conjugated BA27 (anti-Aβ1–40, specific for Aβ40) or BC05 (anti-Aβ35 43, specific for Aβ42). Color was developed with 3,3′,5,5′-tetramethylbenzidine and evaluated at 450 nm with a microplate reader (Molecular Devices, CA). Synthetic Aβ40 and Aβ42 (Sigma, St Louis, MO) of known concentration (estimated from the amino acid composition) were used as standards. The plates were normalized as to each other by inclusion of three standard plasma samples on all plates.

Statistical analysis

Allele frequencies were calculated by allele counting. To evaluate deviation from the HWE of each SNP marker, we carried out an exact test (62) based on the probability of occurrence of genotypic contingency tables with fixed total numbers of alleles within each sample set (LOAD patients and controls included in two screening sets, Exploratory and Validation). For single SNP case–control analysis, the allelic distributions in LOAD patients and controls were compared by means of χ^2 tests via standard 2×2 contingency tables. Evidence of replication, rather than multiple testing corrections, was used to evaluate the significance of associated SNPs. To comprehensively assess the reproducible SNPs, we conducted a Mantel–Haenszel test, where Exploratory and Validation samples in our case–control study were considered as the strata (63), and computed pooled ORs with 95% CI and *P*-values from Mantel–Haenszel statistics (Statcel 2; OMS, Tokyo, Japan). Estimation of haplotypes and their frequencies was carried out for LOAD patients and controls separately by the maximum-likelihood method from unphased diploid genotype data using an EM algorithm (64) with the following parameters: iteration counter, 5000; conversion criterion, 0.000001. To assess the differences in haplotype distribution between LOAD patients and controls, a permutation test (65) was performed. In this test, all permutation *P*-values were empirically computed using 10 000 iterations of random sampling with fixed total numbers of both LOAD and control subjects. OR (95% CI), as an estimate of the relative risk of disease, of each marker or haplotype was calculated from a 2×2 contingency table. For all statistical methods mentioned above, except the Mantel–Haenszel test, we used SNPAlyze software versions 3.2.3 or 6.0.1 (DYNACOM, Chiba, Japan; http://www.dynacom.co.jp/). For calculation of LD measures (D′) and LD block definition by Gabriel *et al.*'s method (66), we used Haploview version 3.32 (67, http://www.broad.mit.edu/mpg/haploview/index.php).

Using SPSS version 13.0 software (SPSS, Chicago, USA), multiple logistic regression analysis (Table 5) was performed to reveal the effects of the *APOE-ε4* [non-carrier of the *ε4* allele (*ε2*2*, *ε2*3* and *ε3*3*)/carrier of the *ε4* allele (*ε2*4*, *ε3*4* and *ε4*4*)], gender (male/female), age and significant SNPs identified here (major-allele homozygote/heterozygote/minor-allele homozygote) on the risk for LOAD as well as their second-order interaction terms. The strength of association between these variables and disease status (control/LOAD) was evaluated with ORs with 95% CI, based on Wald statistics. We examined the four variables by means of a two-step multiple logistic regression analysis according to Akazawa *et al.* (68). In order to examine which variables explain an association with LOAD independently, we initially carried out stepwise logistic regression analysis (forward selection method) without interaction terms. A significance level of 0.05 was used to enter a variable in the model. Through this analysis, the following multiple logistic regression model was fitted (Model 1 in Table 5): $\log(P/(1-P)) = \alpha + \beta_1 X1 + \beta_2 X2 + \beta_3 X3 + \beta_4 X4$, where P denotes the probability of having LOAD, α is the intercept, β_i represents the estimated parameters and Xj the independent variables ($X1$, *APOE-ε4*; $X2$, gender; $X3$, age; $X4$, SNP). We next analyzed the four variables including their second-order interaction terms (SNP_gender, SNP_*APOE-ε4*, SNP_age, gender_*APOE-ε4*, gender_age and age_*APOE-ε4*) by means of a forward stepwise regression method with a significance level of 0.05 for the inclusion of a variable in the model. As a result, the following model was fitted (Model 2 in Table 5): $\log(P/(1-P)) = \alpha + \beta_1 X1 + \beta_2 X2 + \beta_3 X3 + \beta_4 X4 + \beta_5 X5 + \beta_6 X6 + \beta_7 X7$, where P denotes the probability of having LOAD, α is the intercept, β_i represents the estimated parameters and Xj the independent variables ($X1$, *APOE-ε4*; $X2$, gender; $X3$, age; $X4$, SNP; $X5$, SNP_gender; $X6$, gender_*APOE-ε4*; $X7$, age_*APOE-ε4*). Subjects with undetermined SNP genotype data were omitted for multiple logistic regression analysis.

The Mann–Whitney *U*-test was applied to compare differences in the levels of Aβ40 and Aβ42, and their ratio (Aβ40/42) between LOAD patients and controls (Prism 4.0b; GraphPad Software, CA, USA). After Bartlett's test for the homogeneity of variances (Statcel 2) and the KS normality test (Prism 4.0b), the effects of three SNP genotypes (minor-allele homozygotes, heterozygotes and major-allele homozygotes) in three sub-groups stratified as to gender (female–male mixture, female or male) were examined as to levels of the plasma Aβ40/42 ratio using two-way ANOVA (Prism 4.0b). To create more normally distributed datasets, the Aβ40/42 ratio was subjected to log transformation [$\log_2$(Aβ40/42 ratio + 1)] before the two-way ANOVA.

The statistical significance was set at $P < 0.05$.

SUPPLEMENTARY MATERIAL

Supplementary Material is available at HMG Online.

ACKNOWLEDGEMENTS

We wish to thank the patients with AD and their families, and the control individuals for their participation in this study, without whom this genetic work would have been impossible. We also thank N. Takei, K. Horigome, M. Hirose, N. Yahata, T. Tsukie, K. Takadono, A. Kitamura, Y. Satoh, A. Hirokawa, T. Hoshino, S. Yanagihara and M. Saitoh for their technical assistance, and N. J. Halewood for critical reading of the manuscript.

The members of JGSCAD who participated in the collection of blood samples from AD patients and controls were as

follows: All authors on the title page: and Akihiko Nunomura, MD, and Shigeru Chiba, MD, Department of Psychiatry and Neurology, Asahikawa Medical College, Asahikawa; Takeshi Kawarabayashi, MD, Department of Neurology, Neuroscience and Biophysiological Science, Hirosaki University, School of Medicine, Hirosaki; Satoshi Takahashi, MD, Department of Neurology, Iwate Medical University, Morioka; Naoki Tomita, MD, Department of Geriatric and Complementary Medicine, Tohoku University Graduate School of Medicine, Sendai; Jyunzo Ito, MD, Alpine Kawasaki, Kawasaki, Miyagi; Haruo Hanyu, MD, Department of Geriatric Medicine, Tokyo Medical University, Tokyo; Shin Kitamura, MD, Second Department of Internal Medicine, Nippon Medical School, Tokyo; Hitoshi Shinotoh, MD, Asahi Hospital for Neurological Disease, Chiba; Hiroyuki Iwamoto, MD, Department of Neurology, Hatsuishi Hospital, Kashiwa; Masahiko Takahashi, MD, Department of Old Age Psychiatry and Memory Clinic, Tokyo Metropolitan Geriatric Medical; Yasuo Harigaya, MD, Department of Neurology, Maebashi Red Cross Hospital, Gunma; Masaki Ikeda, MD, and Masakuni Amari, MD, Department of Neurology, Gunma University Graduate School of Medicine, Maebashi; Takeo Takahashi, MD, Ina Neurological Hospital, Ina; Ryoichi Nakano, MD, and Masatoyo Nishizawa, MD, Department of Neurology, Brain Research Institute, Niigata University, Niigata; Takeshi Ikeuchi, MD, and Osamu Onodera, MD, Department of Molecular Neuroscience, Bioresource Science Branch, Center for Bioresources, Brain Research Institute, Niigata University, Niigata; Masaichi Suga, MD, Higashi Niigata Hospital, Niigata; Makoto Hasegawa, MD, Niigata Shin-ai Hospital, Niigata; Yasuhiro Kawase, MD, Kawase Neurology Clinic, Sanjo; Kenichi Honda, MD, Honda Hospital, Uonuma; Toshiro Kumanishi, MD, and Yukiyosi Takeuchi, MD, Niigata Longevity Research Institute, Shibata; Atsushi Ishikawa, MD, Department of Neurology, Brain Disease Center, Agano Hospital, Agano; Masahiro Morita, MD, Department of Psychiatry, Mishima Hospital, Mishima; Fumihito Yoshii, MD, Department of Neurology, Tokai University School of Medicine, Isehara; Hiroyasu Akatsu, MD, and Kenji Kosaka, MD, Choju Medical Institute, Fukushimura Hospital, Toyohashi; Masahito Yamada, MD, and Tsuyoshi Hamaguchi, MD, Department of Neurology and Neurobiology of Aging, Kanazawa University Graduate School of Medical Science, Kanazawa; Satoshi Masuzugawa, MD, Department of Neurology, Mie Prefectural Shima Hospital, Shima; Takeo Takao, MD, and Nobuko Ota, Kurashiki Heisei Hospital, Kurashiki; Ken Sasaki, MD, Yoshikatsu Fujisawa, MD, and Kenji Nakata, MD, Kinoko Espoir Hospital, Kasaoka; Ken Watanabe, MD, Watanabe Hospital, Tottori; Yosuke Wakutani, MD, and Kenji Nakashima, MD, Department of Neurology, Institute of Neurological Science, Tottori University, Yonago; Toshiyuki Hayabara, MD, Iwaki Hospital, Kagawa; Terumi Ooya, Town Office, Oonan, Shimane; Mitsuo Takahashi, MD, Department of Clinical Pharmacology, Fukuoka University, Fukuoka; Tatsuo Yamada, MD, Fifth Department of Internal Medicine, Fukuoka University, Fukuoka; Taihei Miyakawa, MD, Labour Welfare Corporation Kumamoto Rosai Hospital, Yatsushiro; Eiichiro Uyama, MD, Department of Neurology, Graduate School of Medical Science, Kumamoto University, Kumamoto; Takefumi Yuzuriha, MD, Department of Psychiatry, National Hospital Organization Hizen Psychiatric Center, Sefuri; and Ryuji Nakagawa, MD, Shizushi Yoshimoto, MD, and Kayoko Serikawa, MD, Ureshino-Onsen Hospital, Saga.

Conflict of interest statement. None declared.

FUNDING

This study was supported by KAKENHI (Grant-in-Aid for Scientific Research) on Priority Areas, Comprehensive Genomics (R.K.), and a Grant-in-Aid for Scientific Research on Priority Areas (C), Advanced Brain Science Project (Y.I.), from the Ministry of Education, Culture, Sports, Science and Technology, Japan, and a Grant for the Promotion of Niigata University Research Projects, Japan (A.M.).

REFERENCES

1. Bachman, D.L., Wolf, P.A., Linn, R., Knoefel, J.E., Cobb, J., Belanger, A., D'Agostino, R.B. and White, L.R. (1992) Prevalence of dementia and probable senile dementia of the Alzheimer type in the Framingham Study. *Neurology*, **42**, 115–119.
2. Hy, L.X. and Keller, D.M. (2000) Prevalence of AD among whites: a summary by levels of severity. *Neurology*, **55**, 198–204.
3. Nakamura, S., Shigeta, M., Iwamoto, M., Tsuno, N., Niina, R., Homma, A. and Kawamuro, Y. (2003) Prevalence and predominance of Alzheimer type dementia in rural Japan. *Psychogeriatrics*, **3**, 97–103.
4. Andersen, K., Launer, L.J., Dewey, M.E., Letenneur, L., Ott, A., Copeland, J.R., Dartigues, J.F., Kragh-Sorensen, P., Baldereschi, M., Brayne, C. *et al.* (1999) Gender differences in the incidence of AD and vascular dementia: The EURODEM Studies. EURODEM Incidence Research Group. *Neurology*, **53**, 1992–1997.
5. Fratiglioni, L., Launer, L.J., Andersen, K., Breteler, M.M., Copeland, J.R., Dartigues, J.F., Lobo, A., Martinez-Lage, J., Soininen, H., Hofman, A. and Neurologic Diseases in the Elderly Research Group (2000) Incidence of dementia and major subtypes in Europe: a collaborative study of population-based cohorts. *Neurology*, **54** (Suppl. 5), S10–S15.
6. Fujishima, M. and Kiyohara, Y. (2002) Incidence and risk factors of dementia in a defined elderly Japanese population: the Hisayama study. *Ann. NY Acad. Sci.*, **977**, 1–8.
7. Kukull, W.A., Higdon, R., Bowen, J.D., McCormick, W.C., Teri, L., Schellenberg, G.D., van Belle, G., Jolley, L. and Larson, E.B. (2002) Dementia and Alzheimer disease incidence: a prospective cohort study. *Arch. Neurol.*, **59**, 1737–1746.
8. Edland, S.D., Rocca, W.A., Petersen, R.C., Cha, R.H. and Kokmen, E. (2002) Dementia and Alzheimer disease incidence rates do not vary by sex in Rochester, Minn. *Arch. Neurol.*, **59**, 1589–1593.
9. Gatz, M., Fiske, A., Reynolds, C.A., Wetherell, J.L., Johansson, B. and Pedersen, N.L. (2003) Sex differences in genetic risk for dementia. *Behav. Genet.*, **33**, 95–105.
10. Maes, O.C., Xu, S., Yu, B., Chertkow, H.M., Wang, E. and Schipper, H.M. (2006) Transcriptional profiling of Alzheimer blood mononuclear cells by microarray. *Neurobiol. Aging*, doi:10.1016/j.neurobiolaging.2006.08.004.
11. Assini, A., Cammarata, S., Vitali, A., Colucci, M., Giliberto, L., Borghi, R., Inglese, M.L., Volpe, S., Ratto, S., Dagna-Bricarelli, F. *et al.* (2004) Plasma levels of amyloid beta-protein 42 are increased in women with mild cognitive impairment. *Neurology*, **63**, 828–831.
12. Wang, J., Tanila, H., Puolivali, J., Kadish, I. and van Groen, T. (2003) Gender differences in the amount and deposition of amyloid beta in APPswe and PS1 double transgenic mice. *Neurobiol. Dis.*, **14**, 318–327.
13. van Groen, T., Kiliaan, A.J. and Kadish, I. (2006) Deposition of mouse amyloid beta in human APP/PS1 double and single AD model transgenic mice. *Neurobiol. Dis.*, **23**, 653–662.
14. Maynard, C.J., Cappai, R., Volitakis, I., Cherny, R.A., Masters, C.L., Li, Q.X. and Bush, A.I. (2006) Gender and genetic background effects on brain metal levels in APP transgenic and normal mice: implications for Alzheimer beta-amyloid pathology. *J. Inorg. Biochem.*, **100**, 952–962.